University of Stavanger

Faculty of Science and Technology

MASTER'S THESIS

Study program/ Specialization: Petroleum Engineering/Production	Spring semester, 2010 Open
Author: I Ketut Oscar Edy	…… (Author's signature)
Faculty supervisor: Helge Hodne External supervisor(s): Arild Saasen	
Title of thesis: Rheological Characterization of Borate Crosslinked Fluids Using Oscillatory Measurements	
Credits (ECTS): 30	
Key words: Rheology Crosslinked Fracturing Fluid Viscoelastic Stimulation Oscillatory Gel	Pages: 63 + enclosure: 10 Stavanger, May 27, 2010

RHEOLOGICAL CHARACTERIZATION OF BORATE CROSSLINKED FLUIDS USING OSCILLATORY MEASUREMENTS

I Ketut Oscar Edy

May 27, 2010

Dedication

This thesis is dedicated to my wife for all the wonderful things she brings to my life and to my parents for their love. I love you.

I Ketut Oscar Edy

ACKNOWLEDGEMENTS

This thesis is the final part of my study for MSc degree in Petroleum Engineering Department at the University of Stavanger, Norway.

First and foremost, I would like to thank my supervisors, Arild Saasen and Helge Hodne, who have been introducing this interesting topic. Their immense support, valuable advices, and guidance throughout the duration of this thesis are highly appreciated. Financial support from Det norske oljeselskap ASA is greatly appreciated. I would also like to thank Halliburton for their fracturing fluids and Kim A. Vorland for his assistance for troubleshooting in experiments.

And last, but not least, I wish to say thank you for my classmates for their support and friendship.

I Ketut Oscar Edy – May 2010

TABLE OF CONTENTS

LIST OF SYMBOLS

a) Latin characters

f	frequency, [Hz]
G^*	complex shear modulus, [Pa]
G'	storage modulus, [Pa]
G''	loss modulus, [Pa]
H	depth, [m]
P_p	pore pressure, [Pa]
P_{bd}	breakdown pressure, [Pa]
t	time, [s]
t_{SG}	gel point, [s]
T_o	tensile strength of rock material, [Pa]

b) Greek characters

α	Biot's poro-elastic constant
γ	strain or deformation, [%] or [1]
γ_A	strain or deformation amplitude, [%] or [1]
γ_L	limiting value of deformation (LVE range, amplitude sweep), [%]
$\dot{\gamma}(t)$	shear rate, [1/s]
δ	phase shift angle, [^{o}]
$\tan\delta$	loss factor or damping factor
η^*, η', η''	complex viscosity and its real and imaginary part, [Pas]
η_0	zero-shear viscosity, [Pas]
ν	Poison's ratio
ρ	the average density of overburden formation, [kg/m^3]
σ_h	total horizontal stress, [Pa]
σ_h'	effective horizontal stress, [Pa]
$\sigma_{h,min}$	minimum horizontal stress, [Pa]
$\sigma_{h,max}$	maximum horizontal stress, [Pa]
σ_{tect}	tectonic stress, [Pa]
σ_v	overburden stress, [Pa]
σ_v'	effective vertical stress, [Pa]
τ	shear stress, [Pa]
τ_A	shear stress amplitude, [Pa]
ω	angular frequency, [1/s]

LIST OF FIGURES

LIST OF TABLES

ABSTRACT

Fracturing fluid has a very important role in hydraulic fracturing treatment. Viscosity of hydraulic fracturing fluid affects transporting, suspending, and deposition of proppant, as well as flow back after treatment. It should also be capable to develop the necessary fracture width to accept proppants or to allow deep acid penetration. Compatibility with formation fluids and material has to be taken into account (Guo et al. 2007).

Rheology of the fracturing fluid is fundamental for hydraulic fracturing design, i.e. prediction of fracture growth and geometry. Accurate measurements and good understanding of rheological properties of hydraulic fracturing fluids are essential for designing and executing an optimum treatment. Failure in selection of fracturing fluid will result in unsuccessful treatment in term of reservoir conditions, oil production, and net present value.

Borate crosslinked fluids have been widely used as a fracturing fluid in the oil industry. Experimental study has been conducted to investigate the rheological properties of borate crosslinked fluids and the results are presented in this paper.

Many oscillatory measurements have been conducted to investigate the behavior of the rheological properties of the fracturing fluid samples under different conditions and the possible relationship among them. Results of the oscillatory measurements of certain borate crosslinked fluids are shown in this paper. It was demonstrated that the linear-viscoelastic-limit and flow-point frequency are dependent on temperature.

PREFACE

This thesis studies the rheological properties of hydraulic fracturing fluids. Fracturing fluids from Halliburton have been tested in the laboratory under different conditions to characterize its rheological properties.

Background

Hydraulic fracturing plays a major role in enhancing petroleum reserves and daily production. In hydraulic fracturing treatment, the fracturing fluid has a very important role because it controls the efficiencies of carrying proppants which filling in the fracture. Viscosity of hydraulic fracturing fluid affects transporting, suspending, and deposition of proppant, as well as flow back after treatment. Certain fracturing fluids could also be incompatible with reservoir fluids and rock. Rheology of the fracturing fluid is fundamental for hydraulic fracturing design, i.e. prediction of fracture growth and geometry. Accurate measurements and good understanding of rheological properties of hydraulic fracturing fluids are essential for designing and executing an optimum treatment. Failure in the selection of fracturing fluid will result in an unsuccessful treatment in term of reservoir conditions, oil production, and net present value (Guo et al. 2007; Gidley et al. 1989; Economides 2007; Economides and Nolte 2000).

Objective

The objective of this work is to study and characterize the rheological properties of certain hydraulic fracturing fluids under different conditions using a Physica UDS 200 rheometer.

Thesis Structure

The thesis is started with general concepts in stimulation treatment especially hydraulic fracturing which are presented in Chap. 1. Description of hydraulic fracturing fluid is given in Chap. 2. The next chapter, Chap. 3, represents the base theories of the laboratory experiments. Results and discussions will take part in Chap. 4. Then conclusion is given based on the results in the study.

CHAPTER 1 INTRODUCTION

Reservoir stimulation and artificial lift are the two main activities of the production engineer in the petroleum and related industries. The main purpose of stimulation is to enhance the property value and/or to increase ultimate economic recovery. The stimulation treatments are intended to remedy, or even improve, the natural connection of the wellbore with the reservoir (Economides and Nolte 2000).

Materials in this chapter were taken from Zolotukhin et al. (2005), Fink (2003), Economides and Nolte (2000), Economides (2007), and Guo et al. (2007).

1.1 Reservoir Justification of Stimulation Treatments

There are two main areas of interest for a stimulation treatment:

1. Wellbore zone and its proximity
2. Rest of a reservoir

Different kinds of stimulation technology are generally used depending on the area of interest:

1. Acid washing
2. Matrix acidizing
3. Acid fracturing
4. Hydraulic fracturing

Stimulation is needed to remove skin zones around the wellbore. The total skin effect is a composite of a number of factors that can be divided into pseudoskin and formation damage as shown in Fig. 1.

Pseudoskin effects are defined as skins that appear due to: 1) limited entry; 2) off-centered well; 3) gas blockage; 4) turbulent flow in the vicinity of a well; 5) collapsed tubing; or 6) poor isolation due to poor cementation.

Formation damage is a result of the following failures:

- Drilling damage due to drilling mud solid invasion and/or drilling filtrate invasion
- Cementing damage due to cement slurry invasion
- Perforation damage
- Damage during production due to precipitation of organic/inorganic material, bridging, and blocking
- Damage during stimulation treatment

Skin analysis has to be performed prior to stimulation treatment.

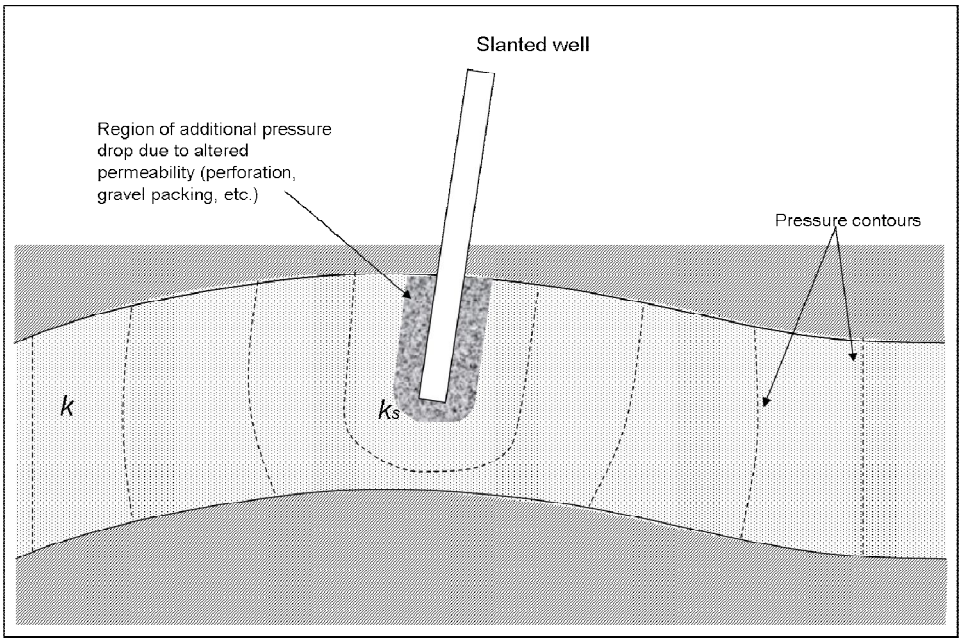

Figure 1 *Skin effect due to converging of flow lines and near wellbore permeability impairment (Zolotukhin et al. 2005)*

1.2 Types of Stimulation Treatment

There are several types of stimulation treatment that can be conducted to remove the skin effect.

Acid washing is a type of stimulation to remove acid soluble scales present in the wellbore or to open perforations. Acid washing is the least expensive of all the near wellbore treatment techniques. A small quantity of acid delivered to the desired position in the wellbore reacts with scale deposits or the formation. Acid may be circulated back and forth across the perforations or formation face.

Matrix acidizing is a type of stimulation to remove near-wellbore damage by injecting acid into the formation. The objective of matrix acidizing is to recover the original reservoir permeability or even create additional permeability (e.g. in carbonate formation). In sandstone formations, the acid attacks the clogging particles. Normally, sandstone formations are treated with hydrochloric/hydrofluoric (HCl/HF) mixtures. In carbonate formations (limestone and dolomite), the acid mainly attacks the matrix itself which creates secondary permeability. Hydrochloric acid is usually used in stimulation treatment of carbonate formations.

Hydraulic fracturing is stimulation treatment by creating fractures to connect the wellbore with the undamaged reservoir. Hydraulic fracturing is usually carried out in formations with low permeability whereas matrix acidizing is performed in medium to high permeability

formations (k > 10 mD). Matrix acidizing treatment is regarded as inexpensive operation as compared to hydraulic fracturing in vertical wells but this is not true for horizontal wells.

In horizontal wells, the long intervals to be stimulated require very large volumes of stimulation fluids with associated pumping times (100 hours and more) and corrosion problems. Thus, sophisticated stimulation techniques such as the application of coiled tubing for diverting the acid are needed. Because the horizontal well trajectory will likely intersect naturally existing fractures, there is also a higher risk of leak-off. The combination of these factors leads to higher risks and costs for application of matrix acidizing in horizontal well.

In this chapter, the discussion is limited and focused on hydraulic fracturing.

1.3 Hydraulic Fracturing

Hydraulic fracturing is a well-stimulation technique that is most suitable to wells in low and moderate permeability reservoirs that do not provide commercial production rates even though formation damages are removed by acidizing treatments. A low leakoff fracturing fluid is essential to reduce the injection rate requirement.

1.3.1 Breakdown Pressure (Guo et al. 2007)

Breakdown pressure is one of the key parameters used in hydraulic fracturing design. The magnitude of this parameter depends on formation depth and properties. Estimation of the breakdown pressure begins with in situ stress analysis.

The in situ stress caused by the weight of the overburden formation in the vertical direction is described as

$$\sigma_v = \frac{\rho H}{144} \tag{1.1}$$

where

σ_v = overburden stress
ρ = the average density of overburden formation
H = depth.

Units in Eq. 1.1 are [psi], [lb/ft^3], and [ft] for σ_v, ρ, and H, respectively. The corresponding units in SI metric are [Pa], [kg/m^3], and [m] for σ_v, ρ, and H, respectively.
The overburden stress is carried by both the rock grains and the fluid within the pore space between the grains. The contact stress between grains is called effective stress.

$$\sigma_v^{'} = \sigma_v - \alpha P_p \tag{1.2}$$

where

σ_v' = effective vertical stress, Pa
α = Biot's poro-elastic constant
P_p = pore pressure, Pa.

The effective horizontal stress is expressed as

$$\sigma_h^{'} = \frac{v}{1-v}\sigma_v^{'}, \tag{1.3}$$

where v is Poison's ratio. The total horizontal stress is then expressed as

$$\sigma_h = \sigma_h^{'} + \alpha P_p . \tag{1.4}$$

The magnitude of the horizontal stress may vary with direction because of the tectonic effect. The maximum horizontal stress may be $\sigma_{h,\max} = \sigma_{h,\min} + \sigma_{tect}$, where σ_{tect} is called tectonic stress.

Based on a failure criterion, Terzaghi presented the following expression for the breakdown pressure (Guo et al. 2007):

$$P_{bd} = 3\sigma_{h,\min} - \sigma_{h,\max} + T_0 - P_p \tag{1.5}$$

where

P_{bd} = breakdown pressure, Pa
$\sigma_{h,min}$ = minimum horizontal stress, Pa
$\sigma_{h,max}$ = maximum horizontal stress, Pa
T_o = tensile strength of rock material, Pa.

The breakdown pressure or formation fracturing pressure is used to predict the breakdown pressure of the formation.

Knowledge of the stresses in a reservoir is needed to get information about this breakdown pressure or fracture initialization pressure.

1.3.2 Rock Mechanics Aspects of Fracture Propagation

Fracture propagations mostly points outward in opposite directions from a wellbore and are oriented more or less in a vertical plane. Normally, fracture propagates in a direction orthogonal to the direction of minimum stress. In a deep well, horizontal stress usually is the minimal; therefore vertical fractures will occur in fracturing.

Typically, fractures propagate:

- in a radial fashion (penny-shaped fracture)
- predominantly, in the lateral section

The penny-shaped fracture development can be observed in the early stage of fracture propagation while the latter is typical for later stages of fracture development.

Fracture propagation is mostly affected by the following factors:

- variation of in-situ stresses existing in different layers of rock

- relative bed thickness of formations in the vicinity of the well
- variations in mechanical rock properties (elastic modulus, toughness, or ductility)
- bonding between formations
- fluid pressure gradient in the fracture
- variation in pore pressure from one zone to the next

The entire fracture design depends on the following fracturing parameters (see Fig. 2):

- fracture length (half-length, x_f)
- fracture width (w)
- fracture conductivity ($k_f w/k$)
- fracture height (h_f)
- azimuth, shape or symmetry about the wellbore

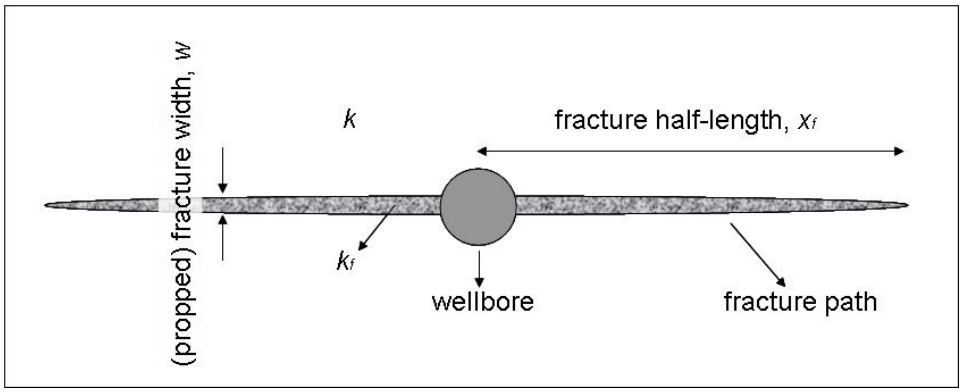

Figure 2 *Typical hydraulic fracturing parameter (Zolotukhin et al. 2005)*

1.3.3 General Considerations in Hydraulic Fracturing Design

Hydraulic fracturing can be divided in two types based on the amount of volume injected (Zolotukhin et al. 2005):

- Mini fracturing, where the volume of fracturing fluid injected is about 2 m^3.
- Massive hydraulic fracturing, where the volume of fracturing fluid injected up to 4000 m^3 with the amount of proppant injected up to $1{,}5 \times 10^6$ kg.

Massive hydraulic fracturing is effective in development of tight (low permeable) gas-bearing formations.

The fracture half-length depends on the type of formations to be stimulated. This is illustrated in Fig. 3 where fracture half-length is plotted on the y-axis while in-situ gas permeability is plotted on the x-axis. It can be seen from Fig. 3 that the tighter the formation is, the longer a fracture can be justified.

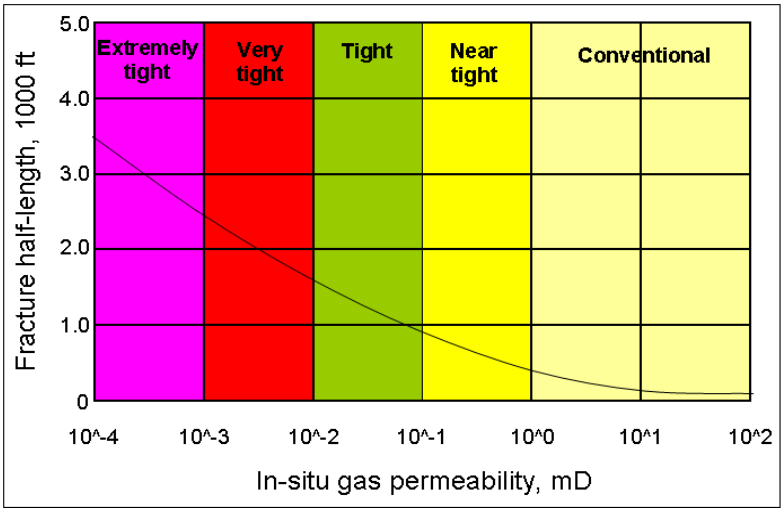

Figure 3 *Fracture half-length for different formations (Zolotukhin et al. 2005)*

McGuire and Sikora presented a significant study of the production increase in a bounded reservoir of area A (acres) for a fracture with a finite conductivity $k_f w$ for the proppant pack, where k_f is the fracture permeability and k is reservoir permeability. The boundary and conductivity effects are summarized in the set of pseudosteady-state curves depicted in Fig. 4. The curves reflect different ratios of the fracture length relative to the drainage radius r_e, with the vertical axis reflecting the folds of increase as J/J_0 and the horizontal axis reflecting dimensionless conductivity based on the drainage radius. The McGuire and Sikora curves were the primary reservoir tool for fracture design and evaluation until the late 1970s (Economides and Nolte 2000). Comparison between hydraulic fracturing vertical well performance and non-stimulated well can be estimated using this figure.

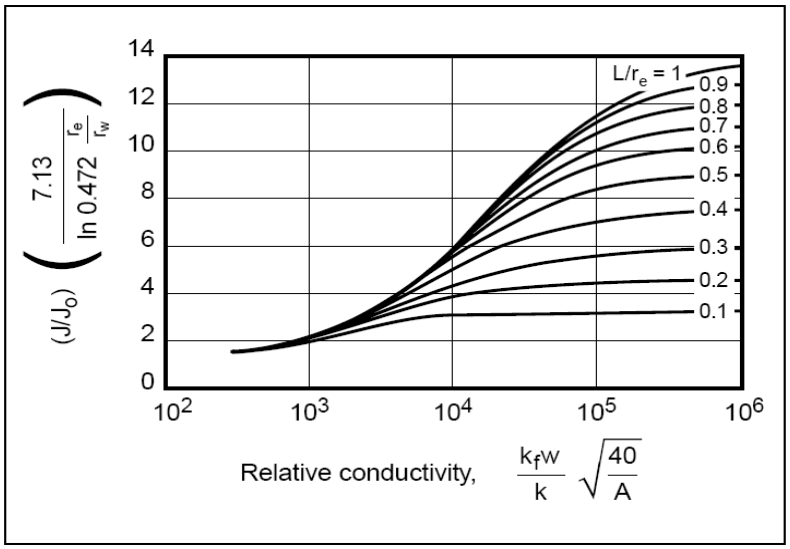

Figure 4 *Performance comparison of pre-treatment and post-treatment productivity indices of a vertical well (Zolotukhin et al. 2005; Economides and Nolte 2000)*

An overall concept for optimization of the hydraulic fracturing design is highlighted in Fig. 5. First, reservoir engineering calculations provide a production forecast for various combinations of fracture half length x_f and conductivity k_fw including the case of no fracture at all. Based on some future price forecast, this allows calculation of a present value, which is the future revenue from the production less future operating costs and discounted back to the present. Hydraulic fracturing calculations based on fluid loss, fracture height, etc., are used to determine the treatment volumes required to generate various combinations of fracture length and propped fracture width, and these calculations are converted into estimated treatment costs. Some form of net revenue economic analysis is then used to determine the best type of proppant, desired fracture length, and other requirements for the optimum treatment (Economides and Nolte 2000).

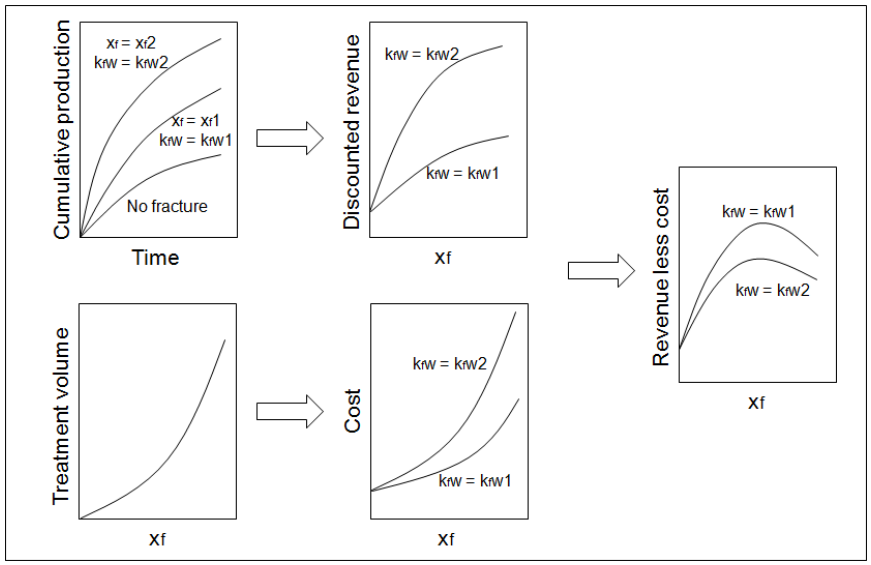

Figure 5 *Hydraulic fracturing design: the total concept for optimization (Economides and Nolte 2000)*

Hydraulic fracturing job consists of the following stages:

- A fracturing fluid is injected into the formation at a rate high enough, given the rheological properties of the fluid, to overcome compressive earth stresses and the rock's tensile stresses. At this pressure the rock fails then allowing a fracture to be formed.
- Continued fluid injection increases the fracture's length and width.
- Proppant injected into the fracture prevents the fracture's closure. It remains open when the well is placed back on production.

The fluid viscosity should decrease after the completion of the fracturing treatment to allow the placement of the proppant and a rapid fluid return through the fracture. Controlling the time at which the viscosity break occurs is very important to avoid proppant flow back.

Hydraulic fracturing designs are performed on the basis of parametric studies to maximize net present values of the fractured wells. A hydraulic fracturing design should follow the following procedure:

1. Select a fracturing fluid
2. Select a proppant
3. Determine the maximum allowable treatment pressure
4. Select a fracture propagation model
5. Select treatment size (fracture length and proppant concentration)
6. Perform production forecast analysis
7. Perform net present value analysis

The properties, types, and additives of fracturing fluid are given in the next chapter.

CHAPTER 2 FRACTURING FLUIDS AND ADDITIVES

The materials in this chapter were taken from Gidley et al. (1989), Fink (2003), Guo et al. (2007), Economides and Nolte (2000), and Economides (2007).

The fracturing fluid is a critical component of the hydraulic fracturing treatment. Its main functions are to open the fracture and to transport proppants along the length of the fracture. Consequently, the viscous properties of the fluid are usually considered the most important. However, successful hydraulic fracturing treatments require that the fluids have other special properties. In addition to exhibiting the proper viscosity in the fracture, they should break and clean up rapidly once the treatment is over, provide good fluid-loss control, exhibit low friction pressure during pumping and be as economical as is practical (Economides and Nolte 2000).

More than 90% of fracturing fluids are water-based according to Fink (2003). The obvious reason is that aqueous fluids are cheaper and can provide control of a broad range of physical properties as a result of additives developed over the years.

The main purposes of additives for fracturing fluids are to enhance fracture creation and proppant-carrying capability and to minimize formation damage.

2.1 Properties of a Fracturing Fluid

The fracturing fluid must have certain physical and chemical properties to achieve successful stimulation.

- It should be compatible with the formation material.
- It should be compatible with the formation fluids.
- It should be capable of suspending proppants and transporting them deep into the fracture but should not carry it back during flow back.
- It should be capable, through its inherent viscosity, to develop the necessary fracture width to accept proppants or to allow deep acid penetration.
- It should be an efficient fluid (i.e., have low fluid loss).
- It should be easy to remove from the formation.
- It should have low friction pressure.
- Preparation of the fluid should be simple and easy to perform in the field.
- It should be stable so that it will remain its viscosity throughout the treatment.
- The fracturing fluid should be cost-effective.

Compatibility is a very critical and necessary characteristic of a fracturing fluid. The treatment will result in a failure if: 1) the chemical nature of the fracturing fluid causes swelling of naturally occurring clays in the formation, thereby plugging pore channels; 2) the fracturing fluid causes migration of fines and/or clays; 3) the fracturing fluids creates emulsions and/or sludging of the crude oil, then plugging rather than stimulation will occur;

4) the fracturing fluid dissolves the cementing material that holds the grains of the sandstone together.

Another important characteristic of a fracturing fluid is its ability to transport the proppants down the tubular goods through perforations and deep into the fracture. To transport proppant and to develop the fracture width needed to create and prop long fractures, high viscosities are needed. Insufficient fracture width from insufficient viscosity will not allow proppants to be transported very far into the fracture.

The ideal fracturing fluid should be efficient with low fluid loss. It is normally attained by combining high fluid viscosity with fluid-loss additives. The fluid-loss additives may consists of plastering agents, bridging agents, microemulsions, or emulsified gas.

Another important characteristic of a fracturing fluid is its ability to revert from high viscosity to low viscosity upon residing in the formation. Viscosity reduction is necessary so that the treating fluid can be removed easily from the formation. The presence of high fluid viscosity in the fracture or in the formation near the fracture can reduce hydrocarbon production. Fracture-fluid viscosity is normally reduced by thermal degradation in high-temperature wells or by controlled degradation through the use of such breaking agents as enzymes, oxidizers, or weak acids. Controlled degradation is essential for the fluid to maintain its viscosity during the treatment but to degrade and lose its viscosity after the treatment. In hydraulic fracturing the fluid is trapped in the area surrounding the fracture and within the fracture itself. This trapped fluid has a negative effect on the relative permeability, effective flow area, and effective fracture lengths which impairs the productivity of well. Penny et al. (2005) studied the formulation and use of a surfactant system formulated into a microemulsion in order to lower capillary pressure and capillary end effects by both lowering interfacial tension between the injected fluid and the gas or oil and the interfacial tension between the injected fluid and the reservoir rock. The microemulsion accelerates the cleanup of injected fluids in tight rock.

Friehauf and Sharma (2009) used a fully compositional fracture simulator to evaluate different design for energized fractures. The results described when to use energized fluids over traditional fluids. It also described the following: 1) choosing the best energizing fluid; 2) importance of leak-off and closure; 3) effect of gas quality; and 4) effect of water sensitivity.

Fracturing fluid systems should have high viscosity but low friction properties. A fluid normally is not acceptable as a fracturing fluid if it cannot be pumped down small tubular goods easily.

A fracturing-fluid should be able to maintain the designed viscosity at bottomhole temperature. A fluid that rapidly loses its viscosity due to thermal thinning or degradation is not applicable for treatment of high-temperature wells. Therefore fracture-fluid stability at high temperature is very critical.

Finally, fracturing fluids should be cost-effective. Economic analysis need to be conducted prior execution comparing the cost and gain.

2.2 Types of Fracturing Fluids

Many different types of fluids have been developed to provide the properties described above because reservoirs to be stimulated vary in temperature, permeability, rock composition, and pore pressure (Economides and Nolte 2000).

Table 1 *Various types of hydraulic fracturing fluids and techniques*

Type	**Remarks**
Water-based fluids	Predominant
Oil-based fluids	Water sensitive; increase the hazard
Alcohol-based fluids	Rare
Emulsion fluids	High pressure, low temperature
Foam-based fluids	Low pressure, low temperature
Noncomplex gelled water fracture	Simple technology
Nitrogen-foam fracture	Rapid cleanup
Complexed gelled water fracture	Often the best solution
Premixed gel concentrates	Improve process logistics
In situ precipitaion technique	Reduce the concentration of the scale-forming ingredients

Table 1 summarizes the various types of fluids and techniques used in hydraulic fracturing according to Fink (2003).

2.2.1 Water-Based Fracturing Fluids

Water –based fracturing fluids have many advantages compared to oil-based fluids.

1. Water-based fluids are economical. The base fluid, water, is much cheaper than oil, condensate, methanol, or acid.
2. Water-based fluids yield increased hydrostatic head compared with oil, gases, or methanol.
3. Water-based fluids are incombustible; hence they are not a fire hazard.
4. Water-based fluids are readily available.
5. Water-based fluids are easily viscosified and controlled.

Linear Fracturing Fluids. Linear fracturing fluids are fracturing fluids without chemical crosslinked structures. The need to thicken water to help transport proppant, to decrease fluidloss, and to increase fracture width was apparent to early investigators. Starch had been used as the first water viscosifiers to thicken and to decrease the fluid loss in drilling mud. Shear sensitivity, lack of temperature stability and bacterial degradation were the reasons behind the short life of this fluid. It was replaced by guar gum in the early 1960's. The guar polymer comes from a bean. When added to water it thickens and viscosifies the fluid. Guar is a naturally occurring polymer that undergoes hydration upon contact with water. The

polymer uncoils, with water molecules attaching themselves to the polymer chain. This creates a viscous fluid by interaction of the polymer coils, one to another, in the water-based system.

Other linear gels used today as fracturing fluids are hydroxypropyl guar (HPG), hydroxyethylcellulose (HEC), carboxymethyl HPG (CMHPG), xanthan gum, and in some rare case, polyacrylamides. HPG was developed primarily to reduce the residue obtained from guar gum and to achieve greater temperature stability. HPG is obtained by the reaction of propylene oxide with the guar molecule, creating a more-temperature-stable, somewhat higher viscosity polymer. The propylene-oxide-groups basically tend to stabilize the polymer against thermal degradation.

A further derivative of guar gum, CMHPG is obtained by the reaction of HPG with sodium monochloroacetate. This product is used only in crosslinked gel applications. This product has lower residue than HPG.

Young et al. (1998) showed that the hydrophobically modified hydroxybutyl guar (HMHBG) has improved properties over native guar, HPG, and hydroxybutyl guar (HBG). It exhibits high viscosities at low shear rates and higher extensional viscosities.

Other viscosifiers used in linear gel systems include HEC, carboxymethylcellulose (CMC), and carboxymethylhydroxyethylcellulose (CMHEC). While guar is usually considered a natural polymer, these cellulose polymers are usually considered synthetics. Cellulose derivatives are formed by reacting natural cellulose from cotton or wood products to form the derivative. HEC is formed by treating cellulose with sodium hydroxide and reacting it with ethylene oxide. Hydroxyethyl groups are introduced to yield a hydroxyethyl ether. CMC is formed by reacting alkali cellulose with sodium monochloroacetate under very controlled conditions. CHMEC is produced by a double derivation, combining the reactions for the creation of HEC followed by the reaction of sodium monochloroacetate with HEC. These products yield high viscosity polymers that have no residue upon degradation.

Another viscosifier is xanthan gum, which is used both as a linear gel system and a crosslinked fluid. Its major use in stimulation has been as a thickener for hydrochloric acid. Its use is limited to acid concentrations up to 15% and temperatures of 200 F (93^{o}C) or less.

The last linear viscosifiers to be discussed are polyacrylamides which primary use is as a friction reducer. These products yield excellent friction reduction at very low concentrations.

Linear gels are relatively simple fluids to use and to control. The problem with linear fluids is their poor proppant suspension capability and their less temperature stability than a similar crosslinked fluid.

A linear gel may be the ideal fluid for a damage-removal treatment or banking-type proppant pack for high fracture conductivity near the wellbore. In order to achieve deep penetration of proppant or of acid away from the wellbore, the higher viscosity crosslinked fracturing fluids are the better option.

Crosslinked Fracturing Fluids. Crosslinked fracturing fluids were considered a major advancement in hydraulic fracturing technology. With linear gels, the only means to obtain increased viscosity is to increase the polymer concentration. Often 80 to 100 lbm polymer/1000 gal (9586 to 11983 g/m^3) water is needed to yield the viscosities necessary to fracture-treat a well successfully with linear gel systems. Adding proppant and dispersing fluid-loss additives into such concentrated solutions of linear fluids is difficult.

Crosslinked fluids eliminated many of the problems when fracture-treating deep hot reservoir using linear gels. The earliest crosslinkers were borates and antimony metal crosslinkers. The metals are dispersed between the polymer strands and an attraction occurs between the metals and the hydroxyl or carboxy groups. This interaction takes a gel system from a true fluid to a pseudoplastic fluid. The borate fracturing fluid was a high pH-system, typically in the pH 10 range, while the antimony was approximately pH 3 to 5.

The first crosslinked fluid was a guar gum system. Many other crosslinker systems have been developed such as aluminium, chromium, copper, manganese, titanium chelates, and zirconium chelates.

Crosslinking the polymer molecule tends to increase the temperature stability of the base polymer. It is theorized that this temperature stability is derived from less thermal agitation of the molecule because of its rigid nature and some shielding from hydrolysis, oxidation or other depolymerization reactions that can occur. Although increasing the apparent viscosity of the fluid by several orders of magnitude, crosslinking of the polymer does not necessarily cause friction pressures to increase to any degree in the pumping operation.

Crosslinking fluids have the tendency to lose viscosity permanently as a result of high shear rates. Because of this, the use of ‘standard’ crosslinked gel systems has declined and have been replaced by delayed crosslinked fracture-fluid systems.

Delayed Crosslink System. This crosslinked systems is a fracturing fluid with a controlled crosslink time which is defined as the time for the base fluid to take on a rigid structure. A delayed crosslinked system allows better dispersion of the crosslinker, yield more viscosity, and improves fracturing-fluid temperature stability. The gel stability is a direct function of crosslinking at low shear rates. The explanation is that at low shear rates the polymer strands are uniformly laid out and crosslinking actually occurs in a very uniform, structured manner, yielding ultimately much higher viscosities and better stability to temperature, hydrolytic and oxidative degradation.

Another advantage of delayed crosslink system is lower pumping friction because of lower viscosity in the tubular goods, thus it can be pumped down more easily.

The main advantages of using a crosslinked fluid than a linear fluid are:

1. Much higher viscosity can be achieved in the fracture with a comparable gel loading.
2. The system is more efficient in fluid loss control.
3. A crosslinked fluid has better proppant-transport capabilities.

4. A crosslinked fluid has better temperature stability.
5. A crosslinked fluid is more cost-effective per pound of polymer.

An example of this system is the borate system. The preparation of borate-crosslinked fracturing fluids is as follows:

1. Introducing polysaccharide polymer into water to produce a gel.
2. Adding an alkaline agent to obtain a pH of at least 9.5.
3. Adding a borate crosslinking agent to crosslink the polymer.

A common borate crosslinking agent can be borax, boric acid, an alkaline earth metal borate or an alkali metal alkaline earth metal borate. The compositions of borate starch are useful for controlling the rate of crosslinking of hydrate polymers in aqueous media for use in fracturing fluids. It can be obtained by reacting starch and a borate source in an aqueous medium to form a borated starch complex. This complex is a source of borate ions, which cause crosslinking of hydratable polymers in aqueous media. It has to be noticed that delayed crosslinking takes place at low temperature condition.

Examples of delayed crosslinking additives are glyoxal, keto aldehydes, hydroxyl aldehydes, glycols and glycerol. Glycols and glycerol can delay the crosslinking of borate in hydraulic fracturing fluids based on galactomannan gum. In this case, the initially formed borate complexes with low molecular weight are exchanged slowly with the hydroxyl groups of the gum which cause delayed crosslinking.

2.2.2 Oil-Based Fracturing Fluids

Using oil-based fracturing fluids is advantageous in certain situations to avoid formation damage to water-sensitive oil-producing formations that might swell if water is introduced. The primary disadvantage of using oil-based fracturing fluids is the fire hazard. Another disadvantage is the higher pumping friction of an oil-based fluid than a delayed, crosslinked water-based fluid system. Pumping pressures are also higher due to lack of hydostatic head of the hydrocarbon compared with water. Additionally, the temperature stability of a delayed, crosslinked water-based system is more predictable in high-temperature well. The preparation and quality control of gelling crude oil require much more care than those of water-based fluids.

2.2.3 Alcohol-Based Fracturing Fluids

Alcohol has frequently been used for the removal of water blocks because alcohol reduces the surface tension of water. In fracturing fluids, alcohol has found wide use as a temperature stabilizer because it acts as an hydrogen scavenger. Methanol based fracturing fluids, particularly at higher concentrations, present difficulty in the controlled degradation of the base fluid. Very high concentrations of any type of breaker are required for complete degradation. The primary benefits of methanol relate to low surface tension, miscibility with water, removal of water blocks, and compatibility with water-sensitive formations.

2.2.4 Emulsion Fracturing Fluids

The two basic types of oil/water emulsions are oil external and water external. An oil-external emulsion is a two-phase system where oil is the continuous phase and water is emulsified in the oil. A water-external emulsion has water as continuous phase and oil as the discontinuous phase.

Water-external emulsions have lower friction pressures because of the low viscosity of water compared with oil. There is a tendency to achieve friction reduction with the polymers in the water phase of water-external emulsion. The pumping pressures of the water-external emulsions are somewhat higher than for typical conventional crosslinked fracturing fluid but much lower than the oil-external emulsions.

2.2.5 Foam-Based Fracturing Fluids

Foam fracturing fluids are simply a gas-in-liquid emulsion. The gas bubbles provide high viscosity and excellent proppant-transport capabilities.

A stable foam has viscous properties similar to a gelled, water-based fluid. The volume of gas necessary to create a stable foam is approximately 60 to 90% of the total volume at a given temperature and pressure. This gives that 60 to 90% of the fracturing fluid is gas. The content of the gas is called quality. Foam stability and viscosity increases from 60 to 90% and revert to a mist above 90%.

Gas bubbles are generated by turbulence when liquid and gas are mixed. The bubbles emulsified in the liquid create foam that will break out slowly with time.

The gas in water emulsion can be stabilized by adding surfactant to coat the gas bubbles. The addition of polymers to the liquid also affects foam stability.

There are several advantages of foam based fracturing fluids. The most obvious are minimizing the amount of fluid placed in the formation and improving recovery of fracturing fluid by the inherent energy in the gas. The inherent energizing capabilities of the fluid caused by entrained gas assist in rapid cleanup or simply promote cleanup in low-pressure formations.

However, foam based fracturing fluids have several disadvantages. Much more care must be taken in running a foam fracturing treatment from a mechanical point of view. Small variations in the water or gas mixing rates can cause the loss of foam stability. Pumping pressures will be large compared with gelled water. It is also very difficult to get high sand concentrations in foam fracturing.

2.2.6 Energizing Fracturing Fluids

A fluid is energized by adding a gas component into the fracturing fluid (Friehauf and Sharma 2009). The advantages of energizing fracturing fluids are quite obvious, particularly

for a formation with low bottomhole pressure. The energy imparted by the gases enables more rapid removal of the stimulation fluid. Entrained gas is also beneficial for fluid-loss control. The incorporation of inert gases into a fracturing fluid will yield proportionally better fluid efficiency than the same fluid without the entrained gases.

The type and characteristics (i.e. solubility) of gas used for energizing a fracturing fluid should be considered carefully. Dissolved gas does not easily dissipate into the formation. When the pressure is subsequently reduced during flowback, the dissolved gas will begin to evolve from the mixture and to impart a solution gas drive to the treating fluid. This gas-drive phenomenon results in effective removal of the treating fluids from the reservoir. It is therefore imperative that a fluid commingled with a gas should be flowed back as quickly as possible.

2.3 Fracturing Fluid Additives

Biocides. A biocide is an additive to maintain gel stability of fracturing fluids on the surface and to protect the formation from bacterial attack. An example of a biocide is *mercaptobenzimidazole*.

Breakers. A breaker is an additive that enables a viscous fracturing fluid to be degraded controllably to a thin fluid that can be produced back out of the fracture. All the breaker systems are used to degrade the polymers in water-based fracturing fluids. Breakers break the molecular chain and thereby effectively lower the molecular weight. Breakers are needed if the temperature is inadequate to cause gel degradation. It is imperative that breakers be included throughout a treatment in such reservoir. Breakers can be run at low concentrations in the early stages of a treatment and increased at later stages to enhance breaking and flowback. The degradation of the treating fluids is needed to achieve maximum well production. Common breakers are enzymes, oxidative and catalyzed oxidative breakers. Oxidative breakers (i.e. alkali, metal hypochlorite, inorganic and organic peroxides) degrade the polymer chains by oxidative mechanisms. Enzyme gel breakers (i.e. xanthan, manan-containing hemicelluloses) degrade the polymer chains by breaking the backbone structure of the thickeners and eventually of the fluid loss additive. Because of their inherent specificity and infinite polymer-degrading activity, enzyme breakers have several advantages to other breaker systems. Enzyme breakers have limitations, despite their advantages, because of interferences and incompatibilities with other additives (e.g. biocides, clay stabilizers, certain types of resin-coated proppants).

Buffers (pH Control Additives). Buffering agents are used in fracturing fluids to adjust and maintain the pH. It also speed up or slow down the hydration of certain polymers. It can be salts of a weak acid and a weak base. Typical products are ammonium, potassium, sodium bicarbonate, fumaric acid, combinations of mono and disodium phosphate, soda ash, sodium acetate or combinations of these chemicals. Another function of a buffer is to ensure that the fracturing fluid is within the operating range of the breakers or degrading agents. Some breakers simply do not function outside specific pH ranges.

Surfactants and Nonemulsifiers. A surfactant (surface-active agent) can be defined as a molecule that seeks out an interface and has the ability to alter the prevailing conditions. Surfactants are included in most aqueous treating fluids to improve the compatibility of the fluids with hydrocarbon-containing formation. Maximum conductivity of hydrocarbon can be obtained when the formation surfaces is water-wet. A surfactant is almost always composed of two parts: a long hydrocarbon chain that is virtually insoluble in water but soluble in oil and a strongly-water-soluble tail. Because there is partial solubility in oil and water, the surfactant will tend to accumulate at the interface of these fluids.

The water-soluble portion of the molecule may be ionically positive (cationic), negative (anionic), or mixed (amphoteric). The ionic charge of the various surfactants used in oilfield stimulation is important in terms of wettability imparted to a given formation. The inherent ionic characteristics of particular formations cause cationic surfactants to leave carbonates water-wet and sandstones oil-wet. Anionic surfactants tend to leave sandstones water-wet and limestones oil-wet. Amphoteric surfactants are organic molecules whose ionic charges depend on the pH of the fluid. The ionic nature of the surfactants is an important consideration and one should be aware of the charge of a surfactant in its selection. It is often useful to select a nonionic surfactant because a large number of formations throughout the world are heterogeneous, limy sands or sandy limes.

An emulsion consists of two immiscible fluids, in which one phase exists as fine droplets dispersed throughout the other phase. Oil field emulsions are either oil in water (where water is the continuous phase) or water in oil (where oil is the continuous phase). If an emulsion is created near the wellbore, severe production blockage may occur.

Surfactant can act as demulsifiers or as emulsifiers because of their surface-active nature. Some fracturing fluids are composed of hydrocarbon and water that are emulsified to build fluid viscosity. If emulsified fluids are used, it is desirable for the surfactant to adsorb on the formation so that the emulsion will break.

Another function of surfactant is to prevent or to treat near-wellbore water blocks. Surfactants lower the surface tension of the water and reduce capillary pressure, which result in lower energy required to move the water across boundaries and through the formation matrix.

Well damage due to blockage by fines (i.e. silts, clay minerals, or drilling-fluids solids) can also be treated by surfactants. If a surfactant that wets the individual fine particles is used in the fracturing fluid, the particles can be removed from the formation more easily when the broken fracturing fluid is produced back.

Huang and Crews (2007) introduced a nanotechnology application for maintaining viscosity at high temperatures and controlling the fluid loss of viscoelastic surfactant fluid, without generating formation damage.

Fluorocarbon Surfactants. Fluorocarbon surfactants are very similar to hydrocarbon surfactants, except that in the oil-soluble half of the molecule, hydrogen atom attached to the carbon chain are replaced by fluorine atoms while the water-soluble portion is effectively unchanged. Fluorocarbon surfactants have advantages over hydrocarbon surfactants: they typically are much more surface-active, and therefore tend to yield lower surface tension at equal concentrations and are useful at low concentrations. In addition to reducing surface tension, fluorocarbon surfactants alter the contact angle at the surface of the pore space. Fluorocarbon surfactants tenaciously adsorb onto the wall of the pore space and cause the contact angle to approach 90^{o}. By effectively reducing capillary pressure to near zero, one can produce the wetting-phase fluid from the formation and fracture more easily.

Clay Stabilizers. Clays and fines present in producing formations may reduce stimulation success. Kaolinite, illite, and chlorite are the most common types found in sandstone reservoirs. The introduction of fracturing fluids or a change in temperature, pressure, or ionic environment may cause the clays to become dislodged and to migrate through the pore system of the rock that may bridge in narrow pore throats and seriously reduce permeability. Susceptibility of a formation to damage by clay swelling ad particle migration appears to depend on the following characteristics: (1) clay content; (2) clay type; (3) clay distribution; (4) pore-size and grain-size distribution and (5) amount and location of cementing material, such as calcite, siderite, or silica. Damage can be mitigated through the use of clay-stabilizing agents. The common clay stabilizers are potassium chloride, ammonium chloride, calcium chloride, and polymeric clay stabilizers.

Fluid-Loss Additives. Hydraulic fracturing concerns in high permeability zones is about damage to the matrix from deeply penetrating fluid leak-off along the fracture or caused by the materials in the fluid that minimize the amount of leak-off. The degree of damage can be minimized if the invasion of the fracturing fluid is minimized. The first priority that has to be considered in fracture treatment design should be maximizing the fracture conductivity. Using high concentration polymer-crosslinked fracturing fluids with fluid loss additives and breakers is recommended in high-permeability fracturing.

To achieve excellent fluid-loss control, one must have not only a bridging material but also a wall-building material. The common fluid-loss additives are guar gum, silica flour, diesel fuel, calcium carbonates and lignosulfonate, and natural starch.

Foamers. Virtually any base fluid can be foamed with a temperature-stable foaming agent. However, nonionic water-soluble surfactants and fluorocarbon surfactant in hydrocarbons often suffer from cloud-point problems at elevated temperatures. Therefore it is desirable to determine that there is no problem with stability of the foamer during the treatment. Common stabilizers for foaming treatments are the basic guar, HPG, and xanthan gum which are added to the fracturing fluid to increase the foam half-life, particularly at elevated temperature.

Friction Reducers. Low pumping friction pressures can be obtained by delaying the crosslinking or adding additives to reduce drag in the tubing. Low viscosity water or hydrocarbon fluids tend to achieve high turbulence which translates into high friction

pressure when pumped at high rates down small tubular goods. When high-molecular-weight polymers are added to these fluids, dramatic decreases in pumping friction are seen because of turbulence suppression. The long-chain polymers blocks turbulence by controlling migration of the individual water molecules, thereby eliminating much of the disorder and turbulence.

The most efficient and cost-effective friction reducers used for fracturing fluids are low concentration of polymers and copolymers of acrylamide. These friction reducers are applicable in water and acid systems. Friction reducers offer no advantages unless the fluid is to be transported in turbulence. High turbulence has to be achieved for the friction reducer to be advantageous, and neither the low-rate casing treatment nor the viscous fluid can be assisted by friction reducers.

Temperature Stabilizers. Temperature stability of fracturing fluids is basically a result of the stability of the base chain polymer, the pH of the fracturing fluid, and/or the presence of oxidizing agents. One means of stabilizing fracturing fluids is to increase the pH into the basic range which is from 8 to 10. Another basic use for temperature stabilizing is removing free oxygen from the system.

Diverting Agents. A diverting agent is typically a graded material that is insoluble in fracturing fluids but soluble in formation fluids. The major purpose of a diverting agent is to divert flow of the fracturing fluid to a zone below or above the zone being treated by plugging off either the perforation (if a cased-hole completion) or some part of the formation (if an openhole completion). The most effective diversion is by ball sealers or zone isolation through packer. The concentration and type of diverting agent are critical.

Scale Inhibitors. It is advantageous that newly made fractures have a scale inhibitor in the fracture to prevent the formation of scale (e.g. calcium carbonate, calcium sulfate, barium sulfate) which may create problems with permeability.

Thickener. Polysaccharides and their derivatives form the predominant group of water-soluble species generally used as thickener to increase viscosity of treating fluids. The increase in fluid viscosity is needed to improve proppant placement and fluid loss control. Examples of thickener are hydroxypropylguar, galactomannans, hydroxyethylcelloluse, carboxymethylcellulose, reticulated bacterial cellulose, and xanthan gum.

Guar. Guar and guar derivatives have been used traditionally to viscosify fracturing fluids. Guar is a branched polysaccharide from the guar plant *Cyamopsis tetragonolobus* with a molar mass of approximately 220,000 Dalton. It consists of mannose in the main chain and galactose in the side chain with ratio mannose to galactose is 2:1. Derivatives of guar are sometimes called *galactomannans*.

Because of their desirable rheologic properties, economics, and ease in hydration, guar-based gelling agents (i.e. hydroxypropylguar) are widely used to viscosify fracturing fluids. Nonacetylated xanthan is a variant of xanthan gum, which develops a synergistic interaction

with guar that exhibits a superior viscosity and particle transport at lower polymer concentrations.

Anionic galactomannans, which are derived from guar gum, have been claimed to be suitable as thickeners. It is capable enhancing viscosities when used either alone or in combination with a cationic polymer and distributed in a solvent.

Boron-crosslinked galactomannan fracturing fluids have higher temperature stability which is the result of addition of a sparingly soluble borate with a slow solubility rate to the fracturing fluid. This polymer also improves the leak-off properties.

Xanthan Gum. Xanthan gum is produced by the bacterium *Xanthomonas campestris*. Xanthans are water soluble polysaccharide polymers. Xanthan gum used in oil field application mostly is in the form of a fermentation broth containing 8% to 15% polymer. Comparing with other polysaccharides, Xanthan's viscosity is less dependent on the temperature.

Concentrates. The fracturing fluid slurry concentrate is useful in producing large volumes of high-viscosity treating fluids at the well site continuously.

Defoamer. Defoamer or anti-foaming agent is chemical additives that reduces and hinders the formation of foam.

2.4 Fracturing Fluid Characterization

Hydraulic fracturing employs special fluids that are intended primarily to create an appropriate fracture geometry while transporting proppants. Key to the entire exercise is the fluid rheology, which affects the fluid viscosity, its proppant-carrying capability, and its propensity for leaking off into the porous medium (Economides and Nolte 2000).

Fracturing fluid systems and additives are characterized for the following objectives (Economides and Nolte 2000):

- additive and system development
- obtaining input data for use in fracture design simulators
- quality control before or during the treatment.

Characterization during the development process for an additive for fluid system is typically used to determine if a new composition is an improvement over an existing system or if it can provide similar performance at a lower cost.

Characterization of fluid systems that obtains representative performance data in critical areas such as rheology, pipe friction pressure, fluid loss rates, fracture conductivity, and formation damage is conducted to obtain data that can be used in fracture design and production simulators.

Characterization of fluid systems at the point of use for quality assurance purposes usually involves methods that can be applied at less than ideal conditions to indicate how the systems are performing.

Whatever the fluid system, a set of data describing the fluid rheology, fluid loss, pipe friction, fracture conductivity, and possible formation damage should be determined before the fluid system is used in field operations (Economides and Nolte 2000).

The rate of fluid leakoff into the formation during a hydraulic fracturing treatment is one of the most critical factors involved in determining fracture geometry for a given treatment design. Further, the rate of fluid leakoff influences fracture closure times and may influence the final distribution of proppant within the fracture. The rate of fluid leakoff to the formation is governed by the fracturing-fluid leakoff coefficient which is a combination of effluent viscosity and relative permeability effect, *Cv*; reservoir-fluid viscosity/compressibility effects, *Cc*; and wall-building effects, *Cw*. The first two coefficients can be calculated from reservoir data and fracturing fluid viscosity. The last coefficient is computed from leakoff data for fluid-loss additives, which must be determined experimentally (Gidley et al. 1989).

Chemistry of borate crosslinked fluids is a function of polymer concentration, borate-ion concentration, pH, and temperature (Kesavan et al. 1993).

The network structure of crosslinked fluids is dependent on the current shear rate, past shear history, and borate ion concentration which in turn depends on pH and temperature (Shah et al. 1997).

The appropriate design of the gel treatment is critical to ensure an efficient gel placement in well completion and workover operations. One important variable of the gel application design is the rheology of the gel system for establishing the crosslinking kinetics and the gel strength after gelation is complete. The viscoelastic properties of gels and gel strength are usually evaluated through dynamic oscillatory measurements. In oil field applications, the determination of the liquid-solid transition (sol/gel transition) of gel system is fundamental. Hydraulic fracturing treatments require the injection of a polymer/crosslinker mixture into reservoir. In these cases, gel point determines the injection period and the penetration of the gel into the rock formation (Romero-Zeron et al. 2004).

CHAPTER 3 MATERIALS AND EXPERIMENTAL THEORIES

The rheology of the fracturing fluid is fundamental for hydraulic fracturing design, i.e. prediction of fracture growth and geometry. Accurate measurements and good understanding of rheological properties of hydraulic fracturing fluids are essential for designing and executing an optimum treatment (Fink 2003; Walters et al. 2001).

Shah et al. (1992) reported that the problem of fluid elasticity is not well understood and characterizing fracturing fluids for their elastic properties is also not very routinely performed.

Accurate rheological characterization of hydraulic fracturing fluids in a laboratory is extremely important prior to their use in the field (Goel et al. 1997).

3.1 Materials

The samples used in this study were borate crosslinked fluids (hydroxypropyl guar polymer hydrated in brine and crosslinked with borate crosslinker) from Halliburton with the following properties:

- Fracturing fluid 1: tailored for 50^{o}C application (3,6 kg of polymer per m^3 of fluid, with surfactant, KCl brine, and pH buffer to a pH of 9,5)
- Fracturing fluid 2: tailored for 100^{o}C application (4,8 kg of polymer per m^3 of fluid, with surfactant, KCl brine, and pH buffer to a pH of 11)

3.2 Rheological Measurements

In this experimental work, the dynamic rheological measurements were conducted using a Physica UDS 200 rheometer with concentric cylinder. The measuring bob radius was 12,5 mm while the measuring cup radius was 13,555 mm. All measurements were performed under oscillatory condition.

Materials in this chapter (Chap. 3.2) were taken from Mezger (2006), Mezger (2002), Barnes (2000), and Barnes et al. (1989).

Oscillatory tests are used to examine all kinds of viscoelastic materials, from low viscosity liquids, pastes, gels, polymer melts to elastomers and rigid solids.

Ideal-elastic behavior

Hooke's law applies when performing oscillatory tests with ideal-elastic materials (i.e. completely stiff, inflexible, and rigid solids).

$$\tau(t) = G^* . \gamma(t) \tag{3.1}$$

Where G* is the complex shear modulus, while τ(t) and γ(t) are the time-dependent values of shear stress and strain (or deformation), respectively. Complex shear modulus, G*, represents the rigidity of the sample or resistance to deformation. If the limit of the linear viscoelastic (LVE) range is not exceeded during the test, then the following relation applies:

$$G^* = \frac{\tau(t)}{\gamma(t)} = const. \tag{3.2}$$

In the LVE range, the τ(t) curve and γ(t) curve are in the same phase in the form of sine curves.

The sinusoidal strain (or deformation) function can be written:

$$\gamma(t) = \gamma_A . \sin \omega t \tag{3.3}$$

Where γ_A [%] is the strain amplitude while ω [1/s] is the angular frequency and is defined as $\omega = 2\pi f$ (f = frequency in Hertz).

The shear rate function, $\dot{\gamma}$(t), is shifted by δ=90° in relation to the γ(t) curve in ideal-elastic behavior. If γ(t) is shown as a sine curve then the $\dot{\gamma}$(t) curve is a cosine curve.

Ideal-viscous behavior

Newton's law applies for ideal-viscous fluids as follows:

$$\tau(t) = \eta^* . \dot{\gamma}(t) \tag{3.4}$$

The complex viscosity, η*, represents the flow resistance of the sample.

The following relation applies in the LVE range:

$$\eta^* = \frac{\tau(t)}{\dot{\gamma}(t)} = const. \tag{3.5}$$

Therefore the τ(t) is always in phase with the $\dot{\gamma}$(t) curve; both run simultaneously as cosine curves if the γ(t) curve is represented as a sine curve. In ideal-viscous samples, a delay of the τ(t) curve in relation to the γ(t) curve occurs with a phase shift angle δ=90°.

Viscoelastic behavior

Presetting:

a) For tests with controlled shear strain as the sine function: $\gamma(t) = \gamma_A . \sin \omega t$ (see Fig. 6)
b) For tests with controlled shear stress as the sine function: $\tau(t) = \tau_A . \sin \omega t$

Measuring result:

a) With controlled strain: τ curve as the phase shifted sine function: $\tau(t) = \tau_A.\sin(\omega t + \delta)$ with the phase shift angle δ between the preset and the result curve (see Fig. 7); sometimes δ is referred to as the loss angle.
b) With controlled stress: γ curve as the phase shifted sine function: $\gamma(t) = \gamma_A.\sin(\omega t + \delta)$.

The shift angle is always between 0^o and 90^o ($0^o \leq \delta \leq 90^o$).

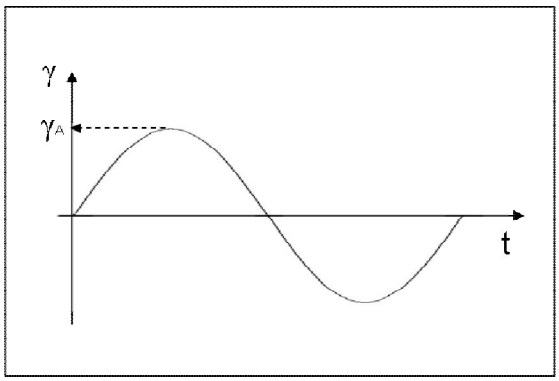

Figure 6 *Preset sine curve with controlled shear strain γ (Mezger 2002)*

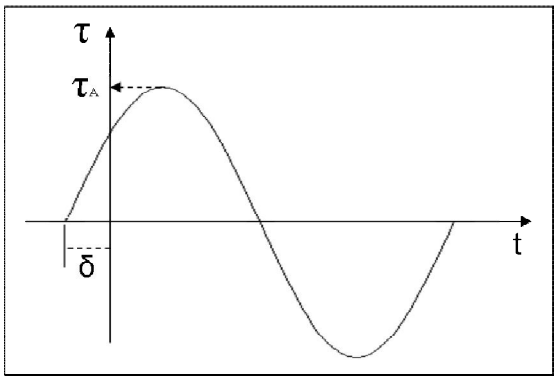

Figure 7 *The resulting sine curve with the phase shift angle δ (Mezger 2002)*

Definition of terms

Definiton of G*, G', G", tan δ, η*, η', and η" are given in this section.

Hooke's law in the complex form:

$$G^* = \tau(t)/\gamma(t) \tag{3.6}$$

where G* is the complex shear modulus with the unit [Pa]. G* could also be calculated from G' and G".

The storage modulus G', with the unit [Pa], is a measure of the deformation energy stored by the sample during the shear process. After the load is removed, this energy is completely available, now acting as the driving force for the reformation process which partially or completely compensates the previously obtained deformation of the structure. Materials which are storing the whole deformation energy are showing completely reversible deformation behavior since they are occurring finally with an unchanged shape after a load cycle. Thus, G' represents the elastic behavior of a sample.

Loss modulus G", with the unit [Pa], is a measure of the deformation energy used up by the sample during the shear process and therefore afterwards, it is lost for the sample. This energy is either used up during the process of changing the sample's structure or dissipated into the surrounding environment in the form of heat. Energy losing materials display irreversible deformation behavior if they occur in a changed form after the load cycle. Thus, G" represents the viscous behavior of a sample.

Loss factor or damping factor ($\tan \delta = G''/G'$) reveals the ratio of the viscous to the elastic portion of the deformation behavior.

In ideal elastic behavior, G' completely dominates G" where $\delta = 0^o$ or $\tan \delta = 0$. In ideal viscous behavior, G" completely dominates G' where $\delta = 90^o$ or $\tan \delta = \sim$.

When G'=G" (meaning viscous and elastic behavior exactly balance) then $\tan \delta = 1$ or $\delta = 45^o$. In the liquid state $\tan \delta > 1$ while in the gel state $\tan \delta < 1$.

The relation among G*, G', G", and δ can be written:

$$|G^*| = \sqrt{(G')^2 + (G'')^2} \tag{3.7}$$

$$\tan \delta = G''/G' \tag{3.8}$$

The descriptions of complex viscosity, its real and imaginary parts are as follows.

Newton's law in the complex form:

$$\eta^* = \tau(t)/\dot{\gamma}(t) \tag{3.9}$$

Where η* is the complex viscosity with the unit [Pas].

The following relation is true for the total amounts: $|G^*| = \omega.|\eta^*|$. (3.10)

The relations among η', η", G', G", and |η*| are as follows:

- Real part of the complex viscosity: $\eta' = G''/\omega$ (3.11)
- Imaginary part of the complex viscosity: $\eta'' = G'/\omega$ (3.12)

- Total amount of complex viscosity: $|\eta^*| = \sqrt{(\eta')^2 + (\eta'')^2}$ (3.13)
- The loss factor: $\tan\delta = \eta'/\eta''$ (3.14)

η' represents the viscous behavior while η" represents the elastic behavior.

In oscillatory tests, the rheometer measures two independent variables: torque, M(t), and shift angle, δ, or deflection angle φ(t) and δ, respectively. From these two raw data, the viscous (G") and the elastic portion (G') of the viscoelastic behavior are calculated.

3.2.1 Amplitude Sweep

Amplitude sweep is defined as an oscillatory test with variable amplitude and constant frequency values.

Description of the test

Presetting:

a) With controlled shear strain (deformation): $\gamma(t) = \gamma_A.\sin\omega t$ with variable strain amplitude γ_A and ω is constant.
b) With controlled shear stress: $\tau(t) = \tau_A.\sin\omega t$ with variable stress amplitude and ω is constant.

Industrial user mostly use ω = 10 1/s as the value of the constant angular frequency (Mezger 2002).

Measuring result:

Usually γ is plotted on the x-axis while both G' and G" are plotted on the y-axis with both axis in a logarithmic scale. Sometimes tan δ is also displayed on the y-axis.

Each of the functions G'(γ) and G"(γ) shows a constant plateau value in the linear viscoelastic (LVE) range at low amplitude. Linear-elastic behavior is found whenever Hooke's law applies: as M_A/φ_A = constant or as τ_A/γ_A = constant (=G*). Linear-viscous behavior is found whenever Newton's law applies: as M_A/ω_A = constant or as $\tau_A/\dot{\gamma}_A$ = constant (=η*).

In the LVE range, the following holds for polymer. $|\eta^*| = \eta_0$.

Analyzing the behavior still in the LVE range, the following relations can be used to describe the "viscoelastic character" of a sample.

a) Gel character, if G' > G"
   Here, the elastic behavior dominates the viscous behavior.
b) Liquid character (sol character), if G" > G'

In this case, the viscous behavior dominates the elastic behavior. The material shows the character of a liquid in the LVE range.

The purposes of amplitude sweeps are mostly to determine the limit of the LVE range. The G' and G" curves show a constantly high plateau value as long as the γ amplitudes remain below the limiting value γ_L, i.e. the structure of the sample is stable under this low-deformation condition. The limit of the LVE range is exceeded at amplitudes higher than γ_L. At this condition, the structure of the sample has already been irreversibly changed or even completely destroyed. Analysis is usually performed in the reversible deformation range using the data from the LVE range only, in which the rheological parameters show constant values. The typical result from amplitude sweep measurement is illustrated in Fig. 8.

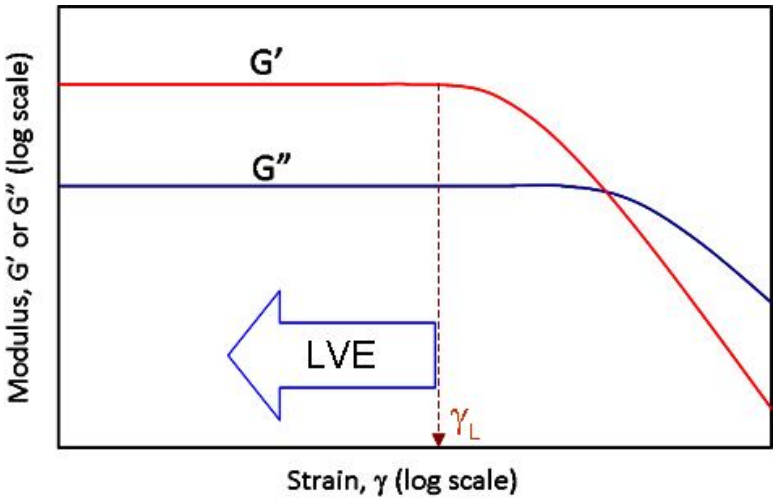

Figure 8 *G'(γ) and G"(γ) with the limiting value γ_L of the LVE deformation range (Mezger 2002)*

Amplitude sweep should always be carried out first on every unknown sample. This is extremely important because if the limit of the LVE range is exceeded in any subsequent test to be performed, then the laws of Hooke and Newton, which are the basis for the largest part of rheology, no longer apply.

3.2.2 Frequency Sweep

Frequency sweep is defined as an oscillatory test with variable frequency and constant amplitude values. In this test, the time-dependent shear behavior is examined. Long-term behavior is simulated by slow movements at low frequencies and short-term behavior is simulated by rapid movements at high frequencies.

The gel behaves like a fluid at low frequencies and like a solid at higher frequencies. The transition from fluid to solid like behavior occurs at a critical frequency that corresponds to the inverse of the relaxation time (Kesavan et al. 1993).

Description of the test

Presetting:

a) With controlled shear strain (deformation): $\gamma(t) = \gamma_A . \sin \omega t$ with variable angular frequency ω= ω(t) and γ_A is constant.
b) With controlled shear stress: $\tau(t) = \tau_A . \sin \omega t$ with ω= ω(t) and τ_A is constant.

The limit γ_L (maximum permissible value of the preset strain) of the LVE range must be determined for each new unknown sample before performing a frequency sweep. The conditions for the frequency sweep can then be selected to ensure that it is carried out in the LVE range.

Measuring result:

Usually log ω or log f is plotted on the x-axis while both log G' and G" are plotted on the y-axis. Sometimes tan δ and or |η*| are displayed on the y-axis.

The most general overall G' and G" response of real examples of structured liquids is shown in Fig. 9.

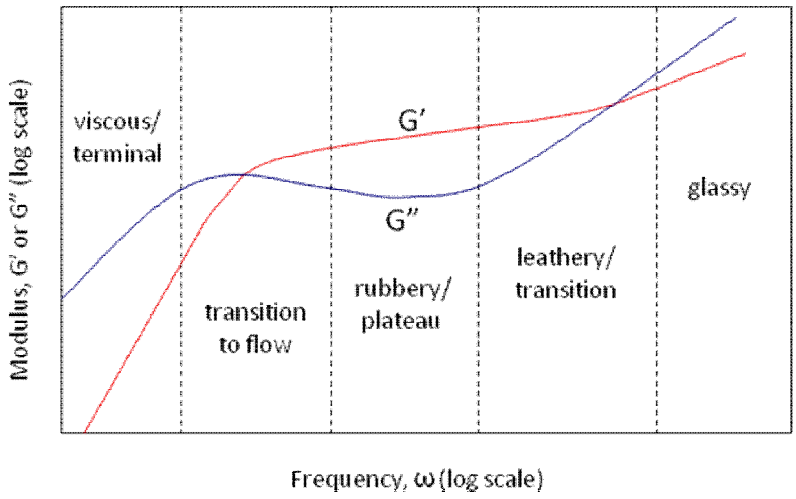

Figure 9 *The various regions in the viscoelastic spectrum of non-Newtonians liquid (Barnes 2000)*

3.2.3 Time Test Oscillation

In this test, both the frequency and amplitude are set at a constant value in each individual test interval. The measuring temperature is also kept constant.

This test examines the time-dependent behavior of samples which form a chemical or physical network during the test period.

The determination of the liquid-solid transition (sol/gel transition) of gel system is fundamental in hydraulic fracturing treatments because gel point determines the injection period and the penetration of the gel into the rock formation (Romero-Zeron et al. 2004).

Description of the test

Presetting:

a) With controlled shear strain (deformation): $\gamma(t) = \gamma_A . \sin \omega t$ with γ_A and ω are constant.
b) With controlled shear stress: $\tau(t) = \tau_A . \sin \omega t$ with τ_A and ω are constant.

Industrial users select ω = 10 1/s = constant for time dependent test oscillation (Mezger 2002).

Measuring result:

Usually, the time t is displayed on the x-axis on a linear scale. Both log G' and log G" are plotted on the y-axis on logarithmic scale.

3.2.4 Temperature Test Oscillation

This type of oscillatory test is carried out at constant dynamic mechanical conditions (both the frequency and amplitude are kept constant in each test interval).

There are two procedures in setting of temperature profile:

1. Linear heating (or cooling) rate in the form of ramp upwards (or downwards).
2. Incremental steps in the form of several test intervals, each with a constant temperature for a certain time period.

This test examines the temperature-dependent behavior of samples undergoing a chemical change during the test period.

Description of the test

Presetting:

a) With controlled shear strain (deformation): $\gamma(t) = \gamma_A . \sin \omega t$ with γ_A and ω are constant.
b) With controlled shear stress: $\tau(t) = \tau_A . \sin \omega t$ with τ_A and ω are constant.

Here, an angular frequency ω = 10 1/s = constant is often selected (Mezger 2002).

Measuring result:

The temperature T is plotted on a linear scale on the x-axis. Both log G' and log G" are usually plotted on logarithmic scale on the y-axis. Sometimes log $|\eta^*|$ and log tan δ (T) over T (on linear scale) are also plotted.

CHAPTER 4 RESULTS AND DISCUSSION

The experimental results obtained from oscillatory measurements (amplitude sweep, frequency sweep, time test oscillation, and temperature test oscillation) are presented and discussed in this chapter.
The presetting of all measurement in this experimental work can be found in Table 2 and 3 in Appendix C. The descriptions of the samples are given in Chap. 3.1.

4.1 Amplitude Sweep

In this series of measurements, the fracturing fluids were subjected to an angular frequency (ω) of 10 1/s based on Mezger (2002). The typical result from this measurement can be seen in Fig. 10 where amplitude strain γ (in fraction) is plotted on the x-axis while both G' and G" are plotted on the y-axis with both axis in a logarithmic scale. Later on, all amplitude strain values on chart are presented in fraction. It is noticeable from Fig. 10 that both curves are increasing from linear before decreasing. This indicates an increasing proportion of the deformation energy (loss modulus G") is being used up to change the structure before the final breakdown takes place (Mezger 2002). Increasing values in G' curve could be a counter to maintain the structure from increasing proportion of the deformation energy.

It can be seen from Fig. 10, the G" curve is considered linear until 100% strain (as a reminder: strain values on chart are in fraction; 1 in fraction equal to 100% in percentage). The G" curve deviated to non-linear at strain approximately 118%. Based on those, it can be concluded for this fracturing fluid under measurement conditions the limit of the LVE range γ_L=118% below which the structure of the fracturing fluid is stable.

Further measurement was immediately performed for the same fracturing fluid presented in Fig. 10 with exactly the same setting configuration to get more information whether the limit of the LVE range was already exceeded. The results, gathered in Fig. 11, demonstrate that the limit of the LVE range has been exceeded since the curves were different. The 'increasing section' on the storage modulus curve after deformation is not appeared in Fig. 11 as in Fig. 10. This could be because of the limit of the LVE range has been exceeded and the structure of the fracturing fluid sample has already been completely destroyed. This condition results in no counter act to maintain the structure from increasing proportion of the deformation energy.

In addition, it can be seen from Fig. 10 and 11 that this fracturing fluid has a gel character (G' > G") under measurement conditions. Here, the elastic behavior dominates over the viscous behavior (Mezger 2002).

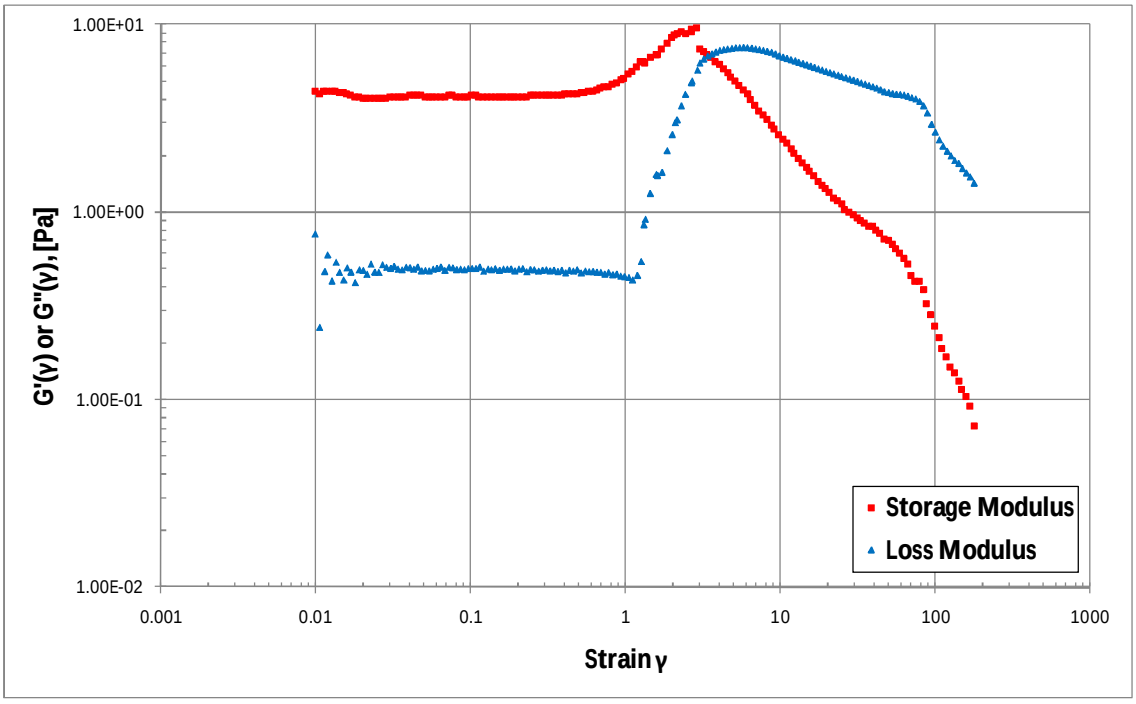

Figure 10 *Typical G'(storage modulus) and G"(loss modulus) curves from amplitude sweep measurement. Here for fracturing fluid 2 at 20°C.*

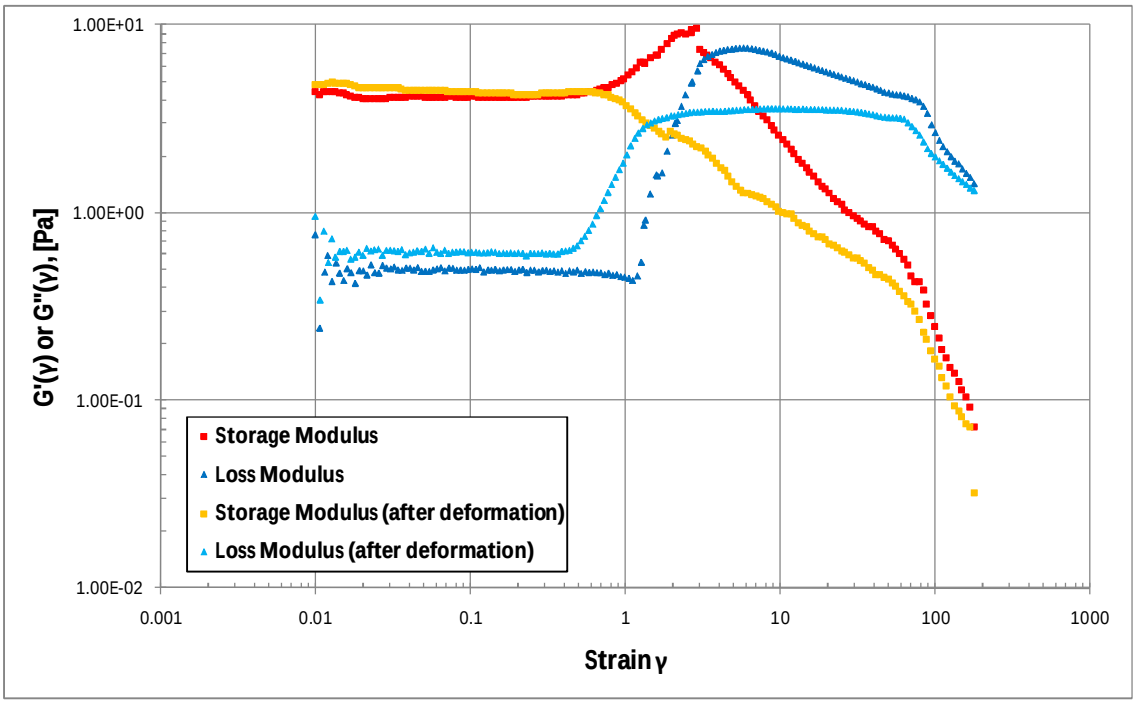

Figure 11 *G'(storage modulus) and G"(loss modulus) curves from before and after deformation. Here for fracturing fluid 2 at 20°C.*

Effect of Temperature and Polymer Concentration

The effect of temperature on limit of the LVE range for fracturing fluid 1 and 2 can be seen in Fig. 12 and 13, respectively. In Fig. 12 and 13, G' and G" are plotted versus strain at different temperature conditions. As the temperature increased, the limit of the LVE range also increased. Fig. 12 and 13 then are separated to Fig. 14, 15, 16, and 17 to get better visualization on the limit of the LVE range.

The effect of temperature and polymer concentration on the limit of LVE range may be better described in Fig. 18 and 19 (as a reminder: fracturing fluid 2 has higher concentration than fracturing fluid 1 as described in Chap. 3.1). In Fig. 18, the G'(γ) function is taken for the analysis for determining the limit of the LVE range. In this method, limit of the LVE range is strain value at which G' started increase continuously before decreasing. In the other hand, the G"(γ) function is taken for the analysis for determining the limit of the LVE range presented in Fig. 19. In this method, limit of the LVE range is strain value at which G" started increase or decrease continuously. The results depicted in Fig. 18 and 19 show that the limit of the LVE range increases when increasing the temperature but decreases when increasing the polymer concentration.

In the view of Fig. 18 and 19, it is noticeable that the plot of the limit of the LVE range (logarithmic scale) versus temperature (linear scale) in semi-logarithmic diagram is reasonably straight line.

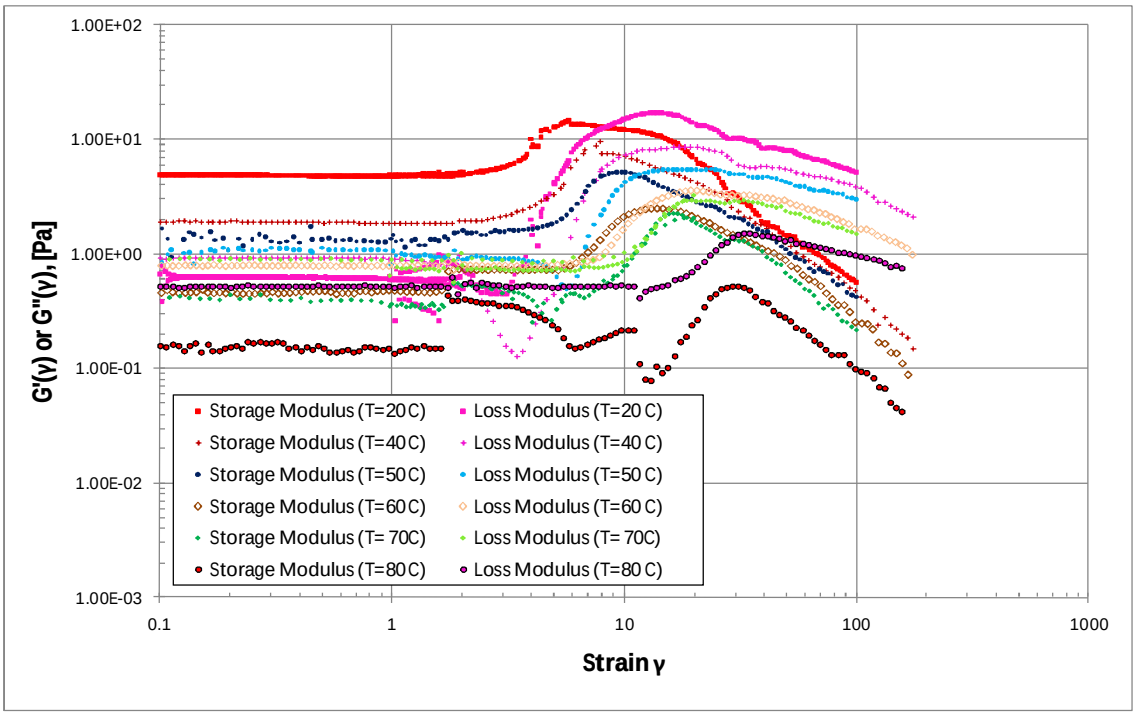

Figure 12 *G' and G" versus strain for fracturing fluid 1 at different temperature*

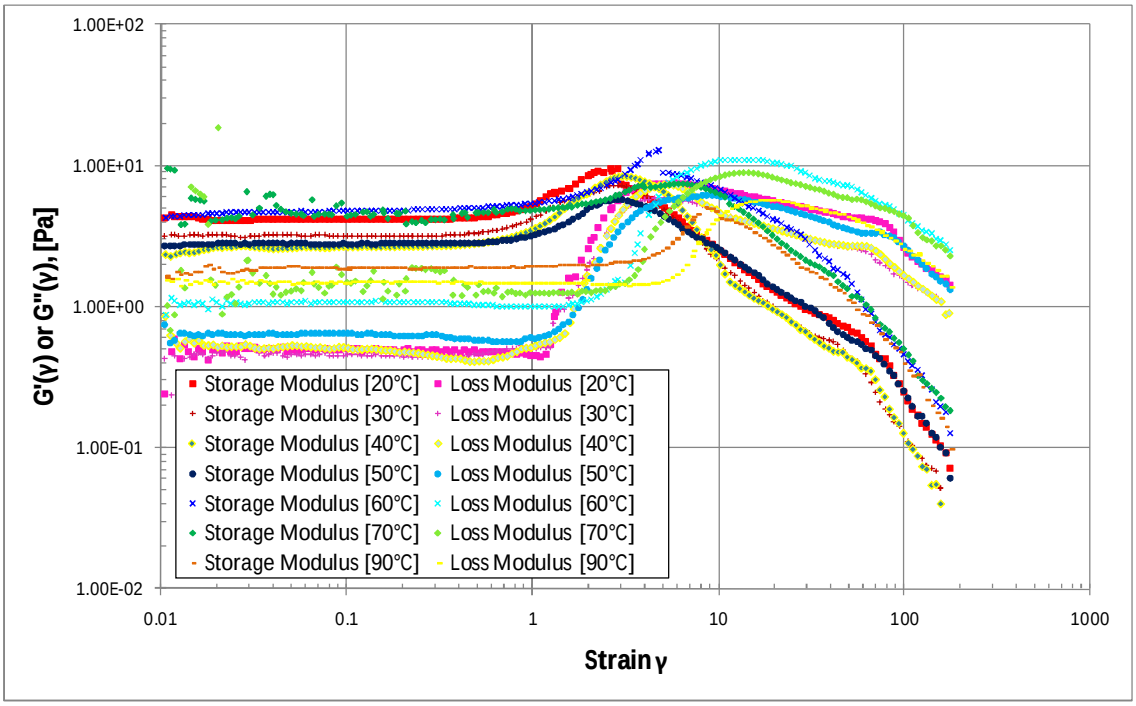

Figure 13 *G' and G" versus strain for fracturing fluid 2 at different temperature*

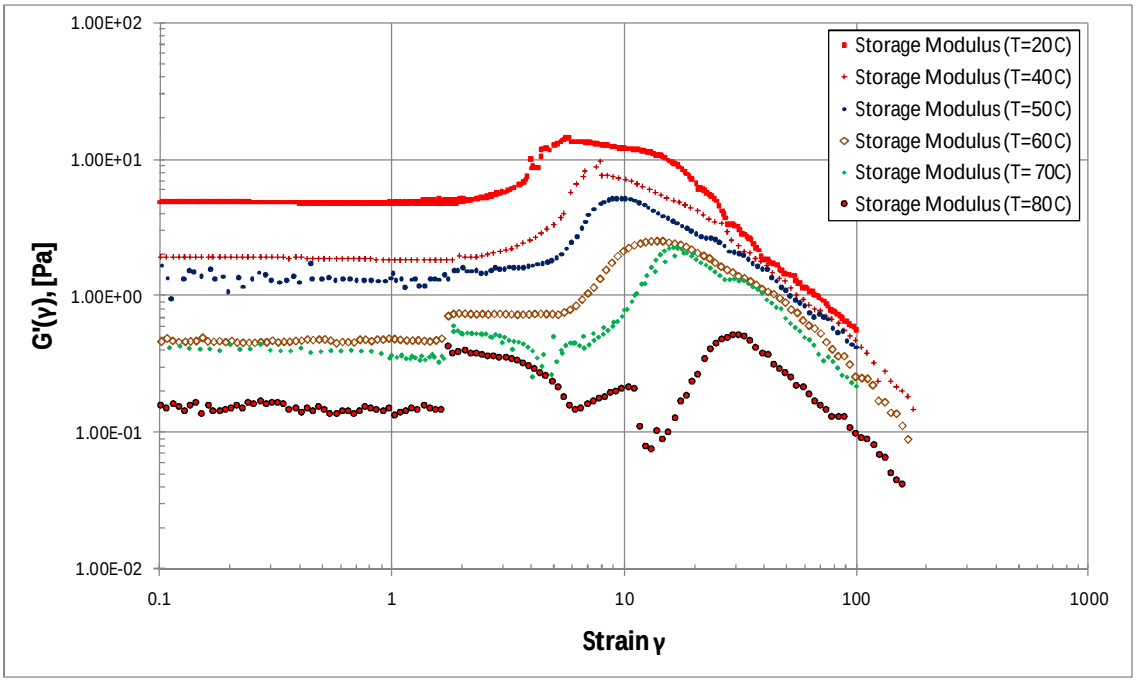

Figure 14 *G' versus strain for fracturing fluid 1 at different temperature*

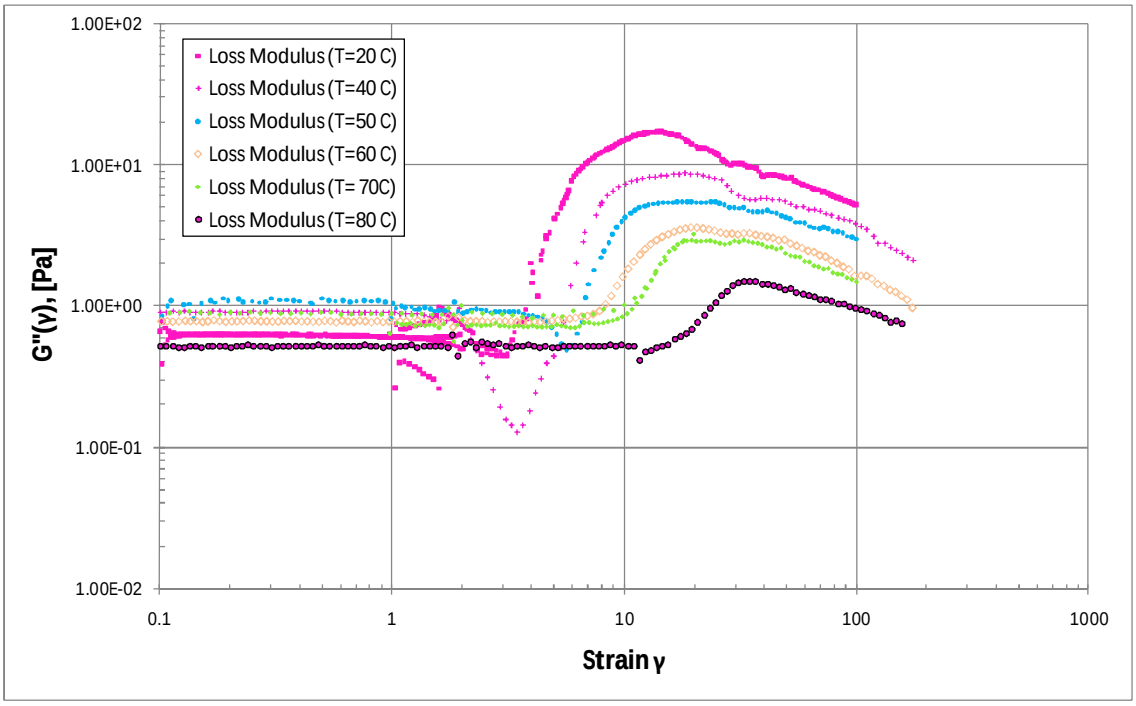

Figure 15 *G" versus strain for fracturing fluid 1 at different temperature*

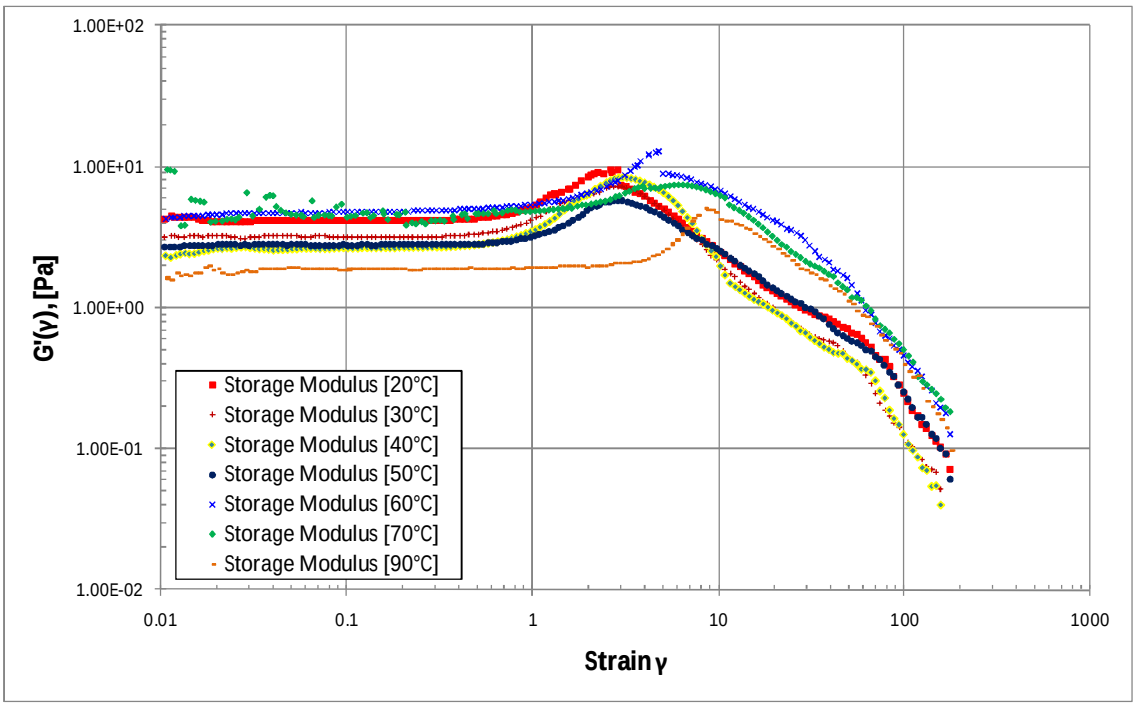

Figure 16 *G' versus strain for fracturing fluid 2 at different temperature*

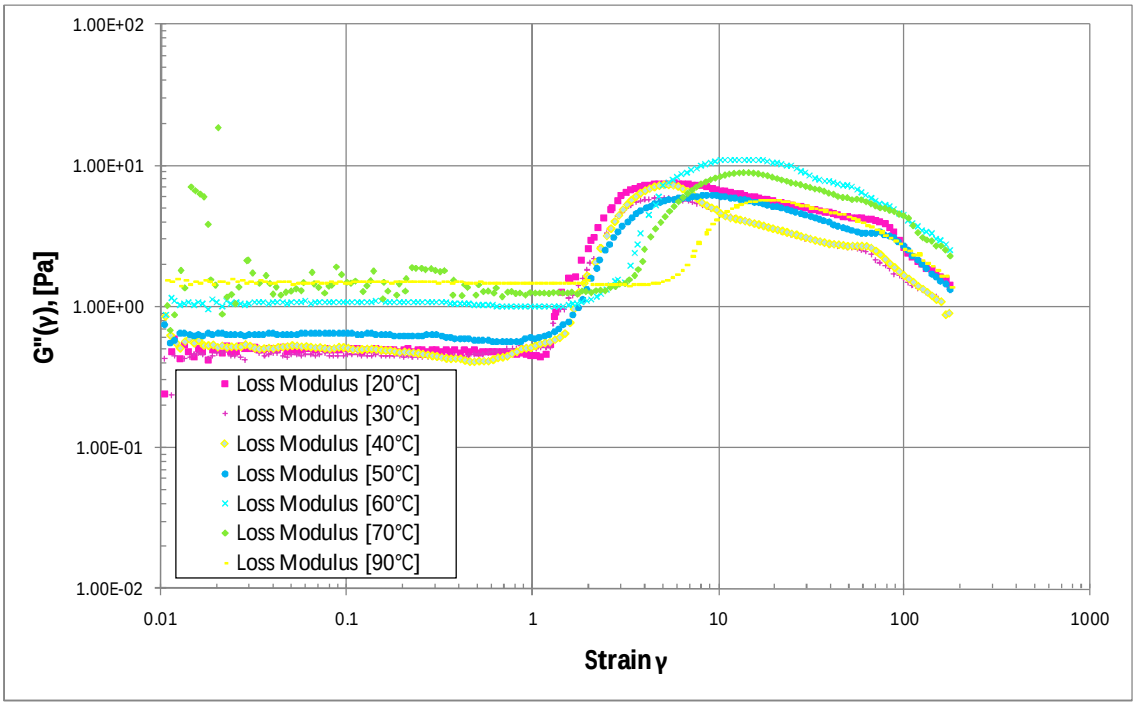

Figure 17 *G" versus strain for fracturing fluid 2 at different temperature*

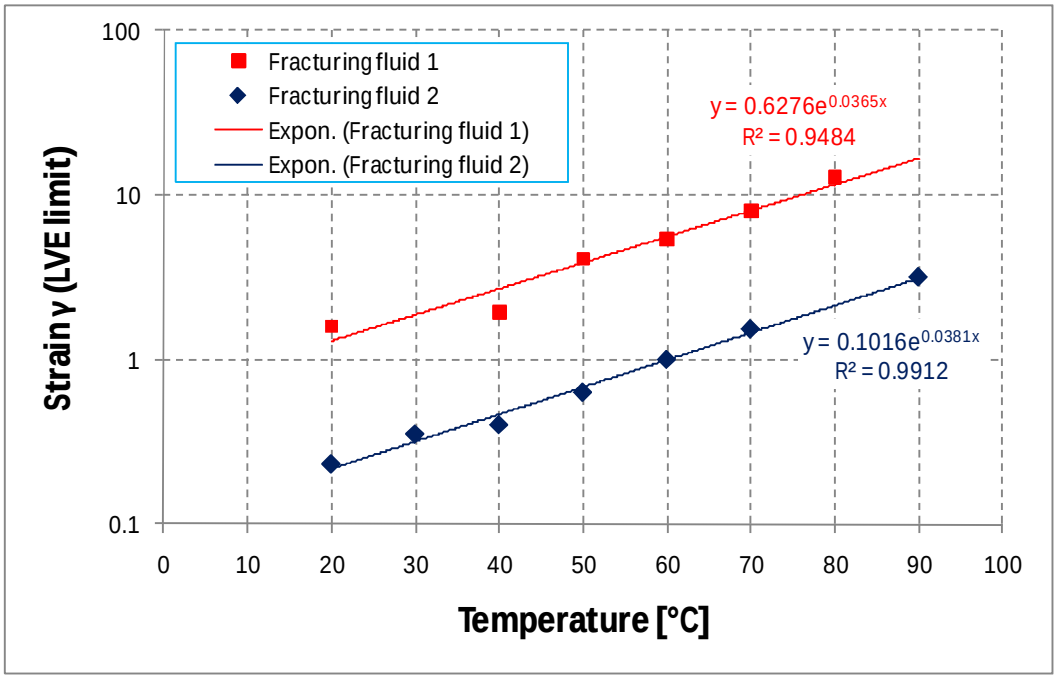

Figure 18 *Limit of the LVE range and polymer concentration versus temperature. Here the G'(γ) function is taken for the analysis for determining the limit of the LVE range. The data fall approximately in straight line.*

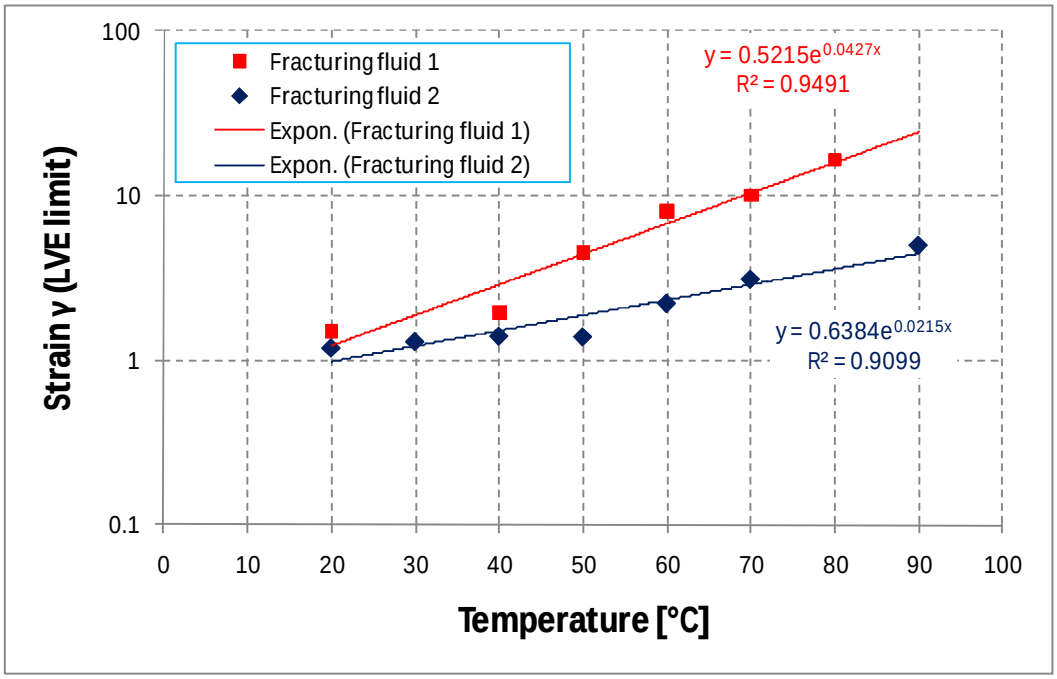

Figure 19 *Limit of the LVE range and polymer concentration versus temperature. Here the G"(γ) function is taken for the analysis for determining the limit of the LVE range. The data fall approximately in straight line.*

Observing Fig. 18 and 19, it is noticeable the dependence of the limit of the LVE range on temperature. The LVE limits for each fracturing fluid on further measurements were taken from the lowest value of the LVE limit from Fig. 18 and 19 at corresponding temperatures.

For example, LVE limit for fracturing fluid 2 at 20^{o}C is 23% (the lowest LVE limit for fracturing fluid 2 at 20^{o}C from Fig. 18 and 19).

In addition, Fig. 12 and 13 give information regarding the character of the fracturing fluids. It is noticeable from Fig. 12 that for fracturing fluid 1 at temperature 20-50^{o}C, the storage modulus (G') is higher than the loss modulus (G") in the LVE range. This conditions means the elastic behavior dominates over the viscous behavior or it shows gel structure. However, at temperature 60-80^{o}C it shows liquid character (sol character) in the LVE range since loss modulus (G") higher than storage modulus (G'). In this condition, the viscous behavior dominates over the elastic behavior. On the other hand, Fig. 13 shows that fracturing fluid 2 has gel structure for all range in temperature measurement (20-90^{o}C) since the storage modulus (G') always higher than the loss modulus (G").

Individual curve for each temperature in amplitude sweep measurement for fracturing fluid 1 and 2 is presented in Appendix A.

4.2 Frequency Sweep

In Chap. 4.1, the maximum permissible values of the preset strain of the LVE range for different temperatures have been determined. In relation with this, the measurements in frequency sweep for fracturing fluid 1 were conducted with amplitude strain 5%, 10%, and 50%. In Fig. 20 the storage modulus (G'), loss modulus (G"), and complex viscosity (η*) are plotted versus angular frequency (ω). In these measurements, the fracturing fluids were tested at temperature 20^{o}C with different setting in steady strain values (5%, 10%, and 50%). It can be seen from Fig. 20 that the data are consistent despite variation in the amplitude strain. It means the measurements were conducted under LVE range as was expected. In other words, amplitude strain of 5%, 10%, and 50% are still within the LVE range for fracturing fluid 1 at 20^{o}C. It is in agreement with Chap. 4.1 where the limit of the LVE range is approximately 150% (1.5 in fraction) for fracturing fluid 1 at 20^{o}C.

Comparing Fig. 9 and 20, a number of specific regions can be differentiated as follows:

a) The viscous or terminal region at very low frequency (long term behavior) at angular frequencies approximately below 0,01 1/s. At this region, the viscous behavior dominates over the elastic behavior (G" > G').
b) The transition to flow region is so called because, when viewed from higher frequencies (where elastic behavior dominates and G' > G"), the loss modulus G", describing viscous or flow behavior, becomes significant (Barnes 2000). This region occurs in interval frequencies approximately 0,1 – 0,01 1/s. The cross over point between the two moduli is at angular frequency 0,025 1/s.
c) The rubbery or plateau region at angular frequencies around 0,1 – 10 1/s. At this region, the elastic behavior dominates the elastic behavior (G' > G"). Since the value of G" is always lower than G', then this fracturing fluid has a gel structure at this region.
d) The leathery or higher transition crossover region at angular frequencies around 10 – 100 1/s. The value of G" rises faster than G' in this region due to high-frequency relaxation and dissipation mechanisms (Barnes 2000). Another crossover frequency can be noticed where angular frequency approximately 50 1/s.
e) Glassy region at highest frequencies is seen at angular frequency higher than 100 1/s. Here, G" again predominates and continues to rise faster than G' (Barnes 2000).

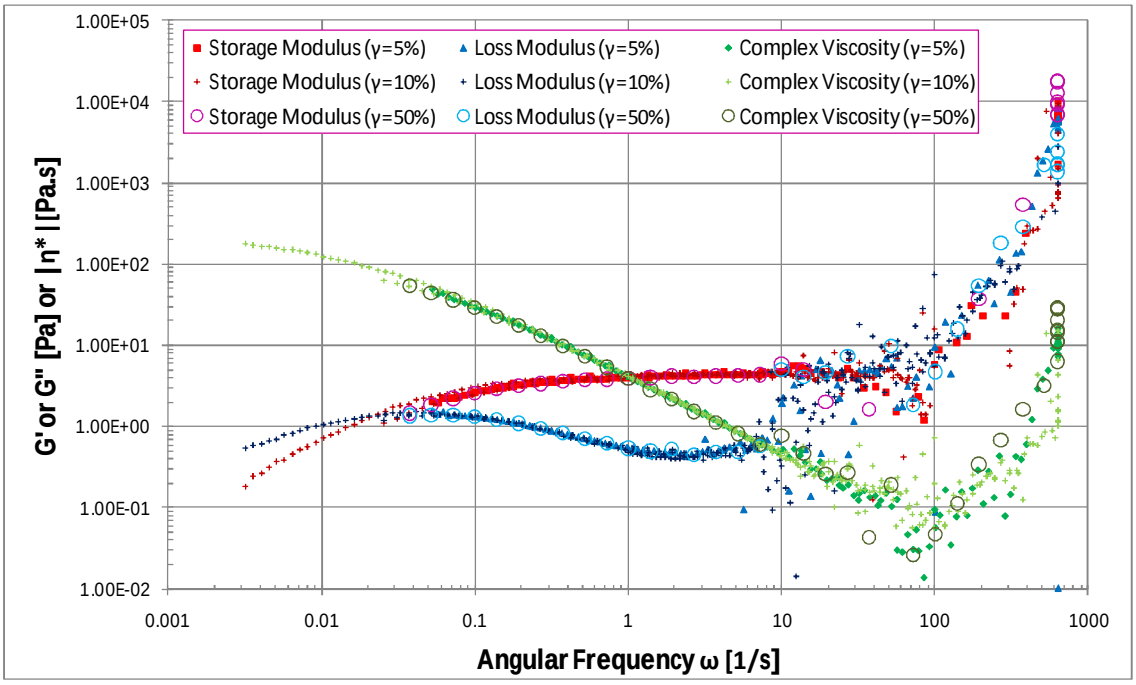

Figure 20 *Frequency sweep result for fracturing fluid 1 at 20°C and different amplitude strain (5%, 10%, and 50%). Storage modulus (G)', loss modulus (G"), and complex viscosity (η*) are plotted versus angular frequency (ω).*

In addition, the following data can be observed from Fig. 20:

- The zero-shear-rate viscosity (η_0) can be obtained at low-enough frequency. Based on relation where $\eta_0 = \lim_{\omega \to 0} |\eta * (\omega)|$ (Mezger 2002), it can be seen that $\eta_0 \approx$ 1,72E+2 Pas (the lowest complex viscosity from the measurements).
- The crossover frequency at which G' = G" is a measure of the longest relaxation time, where relaxation time approximately 40 seconds (inverse of the angular frequency ω = 0,025 1/s) (Barnes 2000).
- The plateau modulus can also be identified from Fig. 20 which is approximately 4,4 Pa. At frequencies above the plateau modulus (and loss modulus minimum), other more complicated mechanisms begin to dictate the values of the moduli as both moduli increase again (Barnes 2000).

The effect of temperature on 'flow-point' could be observed in frequency sweep measurement. The flow-point in here is defined as the angular frequency at which G'=G" when viewed from higher to lower frequencies (transition point from G'>G" to G">G'). This point shows transition from elastic-dominated to viscous-dominated. In these series of measurements, the fracturing fluids were subjected to steady strain of 10% with variation in temperature (20, 50, and 70°C for fracturing fluid 1 and 20, 30, 40, 50, 60, 70, and 90°C for fracturing fluid 2). The results are presented in Fig. 21 and 22 for fracturing fluid 1 and 2, respectively.

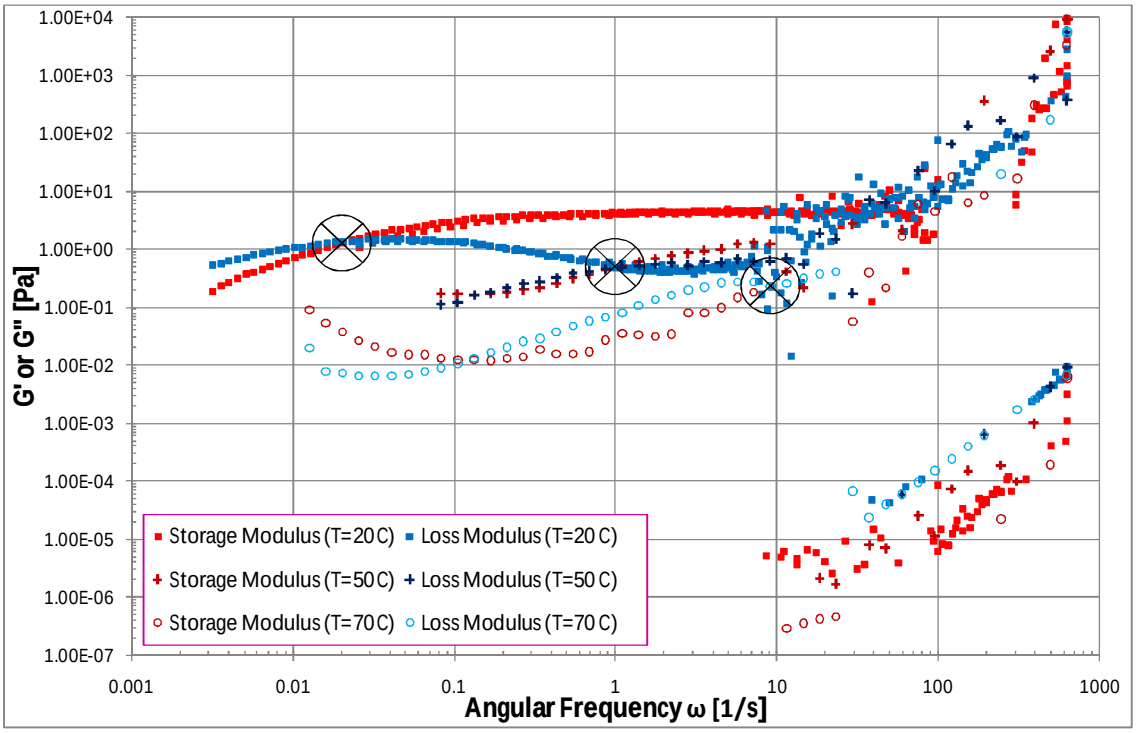

Figure 21 *Frequency sweep result for fracturing fluid 1 at different temperature (20, 50, 70°C). This results show the effect of temperature on the flow-point.*

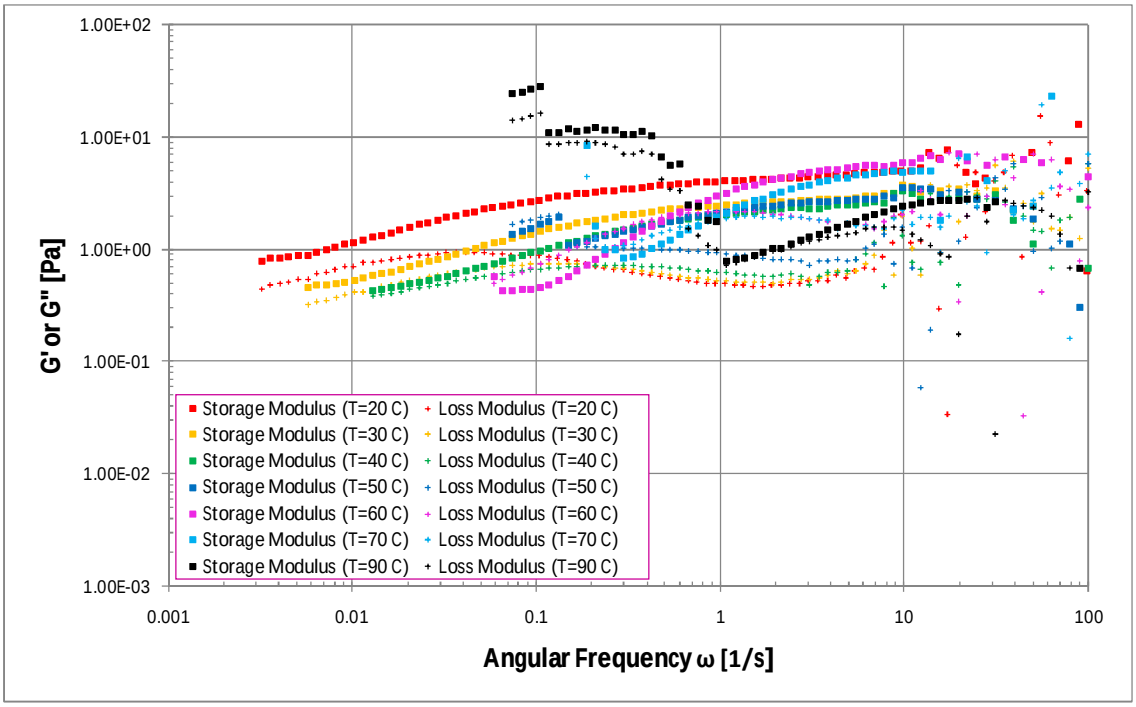

Figure 22 *Frequency sweep result for fracturing fluid 2 at different temperature (20, 30, 40, 50, 60, 70, 90°C). This results show the effect of temperature on the flow-point.*

Despite the noisy data above frequency 10 1/s, it can be seen from Fig. 21 and 22 that the crossover point at 'flow-point' moves to higher frequencies (which mean shorter time). This could be because of increasing in temperature results in higher effect of the 'viscous-part' in the viscoelastic fluid. This observation may be better explained in Fig. 23. The results presented in Fig. 23 show that the flow-point frequency increases when increasing the temperature. It can be seen that the plot of the flow point frequency (logarithmic scale) versus temperature (linear scale) in semi-logarithmic diagram is reasonably straight line.

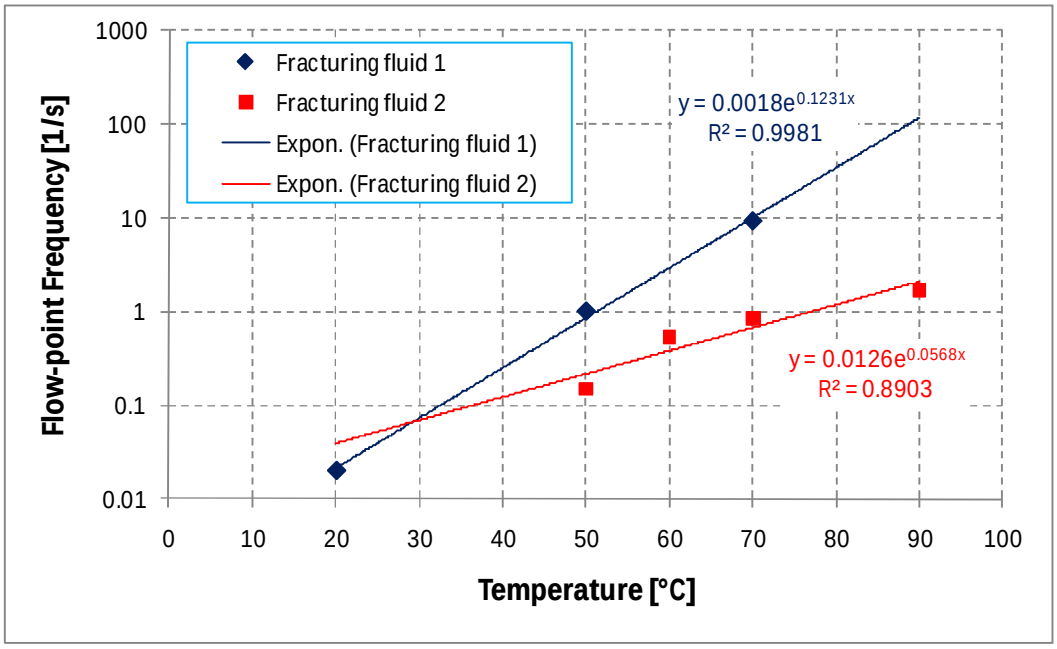

Figure 23 *Flow-point frequency versus temperature for fracturing fluid 1 and 2. The data fall approximately in straight line.*

It can also be observed from Fig. 21 and 22 that the values of both G' and G" increase again at low frequencies for certain temperature. Based on these observation where $\lim_{\omega \to 0} G'(\omega) \neq 0\ Pa$ *and* $\lim_{\omega \to 0} G"(\omega) \neq 0\ Pa$, then these fracturing fluids have chemically cross-linked molecules (Mezger 2002).

Individual curves for frequency sweep measurements for fracturing fluid 1 and 2 can be found in Appendix B.

4.3 Time Test Oscillation

In this test, both the frequency and amplitude are set at a constant value in each individual test interval. The measuring temperature is also kept constant.

In Fig. 24 the storage modulus (G'), loss modulus (G"), and tan δ are plotted versus time. In this series of measurements, fracturing fluid 1 was subjected to frequency 10 1/s at temperature 20°C. This test consists of three intervals with different amplitude strain 1%, 5%, and 10% where time duration for each interval is 120, 120, and 60 minutes respectively.

Despite the noisy data for first interval with amplitude strain 1%, it is obvious from Fig. 24 that this fracturing fluid sample has time-independent or stable structure with constant structure strength under test conditions where the elastic behavior dominates over viscous behavior (G' > G").

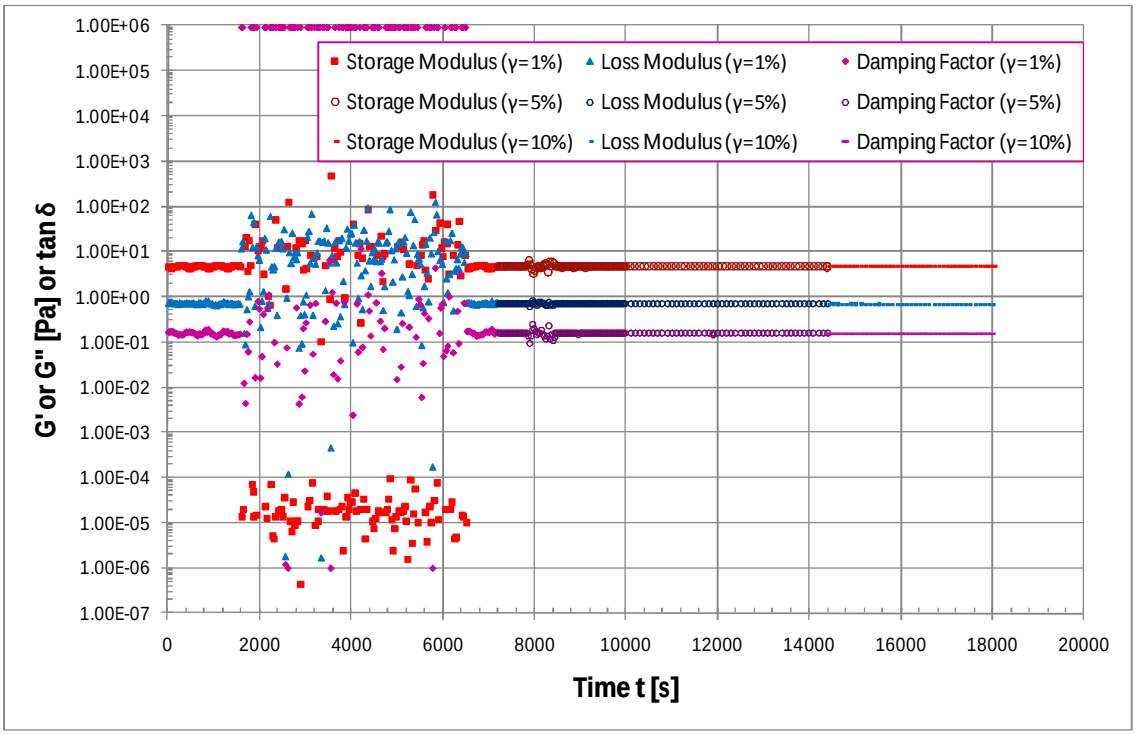

Figure 24 *Time test oscillation result for fracturing fluid 1 at 20°C with variation in amplitude strain (1%, 5%, 10%). G', G", and tan δ versus time.*

Time independent behavior, despite variation in amplitude strain, also confirmed result from Chap. 4.1 regarding LVE range. It means the amplitude strain used in this test (1%, 5%, and 10%) are still within the LVE range.

Similar measurement setting with Fig. 24 has been performed at 50°C with 15 minutes time duration for each interval. The results, gathered in Fig. 25, demonstrate time independent behavior and strain-independent as long as within the LVE range. In this temperature (T = 50°C), the noisy data is appeared at strain amplitude 1% and 5%.

Based on observation from Fig. 24 and 25, next measurements were conducted under single amplitude strain 10%.

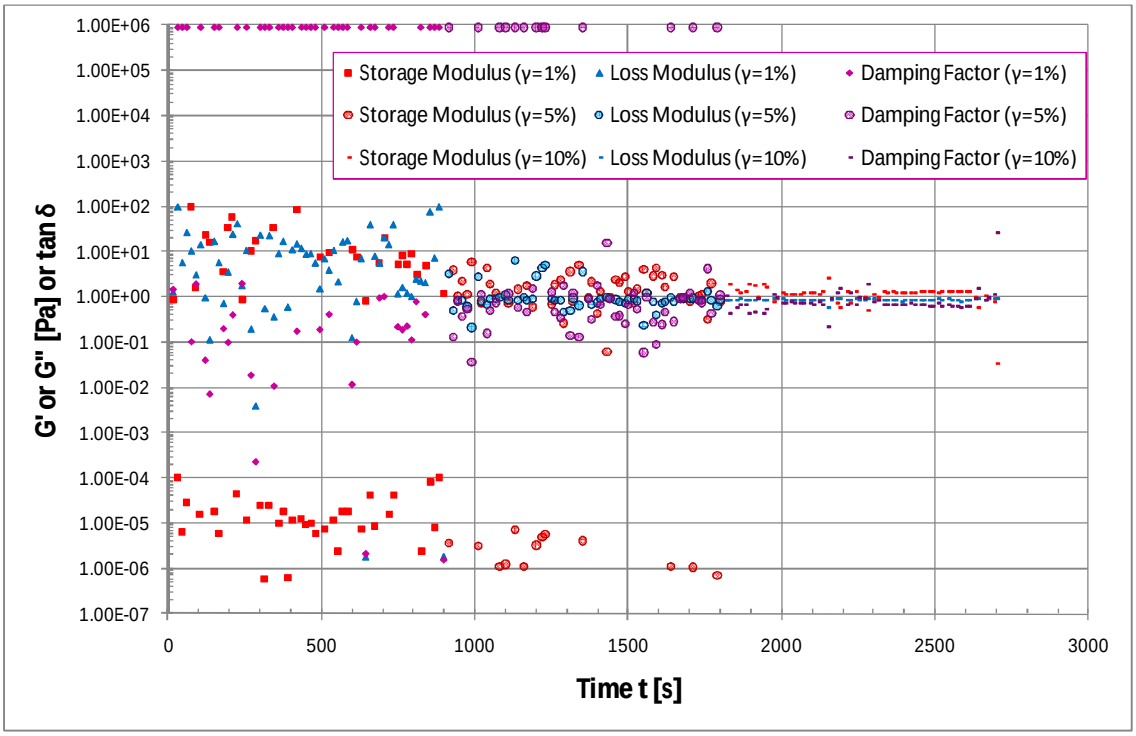

Figure 25 *Time test oscillation result for fracturing fluid 1 at 50°C with variation in amplitude strain (1%, 5%, 10%). G', G", and tan δ versus time.*

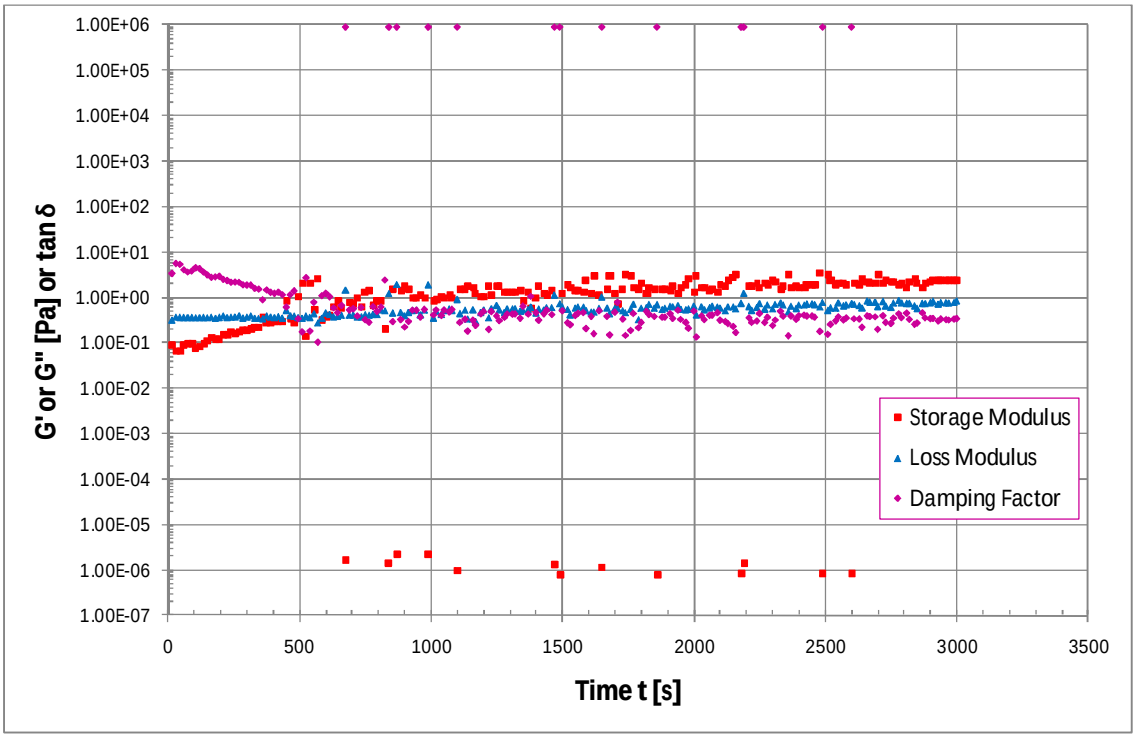

Figure 26 *Time test oscillation result for fracturing fluid 1 at 90°C with 10% amplitude strain. G', G", and tan δ versus time.*

The next experiments were performed at 90°C, during 50 minutes, angular frequency 10 1/s, and 10% amplitude strain. The results, presented in Fig. 26, show the response changes from a loss-modulus-dominated viscous situation at short times, to a storage-modulus-dominated elastic situation at long times. Hardening of this fracturing fluid sample can also be observed from Fig. 26. It examines the time-dependent behavior of sample which forms a chemical or physical network during the test period.

For gel formation processes, the interval in which G" > G' is referred to as the sol state (liquid state), and the interval in which G' > G" is referred to as the gel state (solid state). The time point at the intersection of the G' and G" curves mark the sol/gel transition point which also called the gel point. At this time point G' = G" or tan δ = G"/G' = 1 (Mezger 2002). From Fig. 26, it can be seen that the time point of the sol/gel transition t_{SG} is approximately 500 s. This fracturing fluid sample displays liquid character when G" > G' up to the time point t_{SG} and can therefore easily be deformed. The cross-linked or gel-like state, which makes the sample form-stable is not reached before the time point t_{SG} is surpassed, when G' > G" (Mezger 2002).

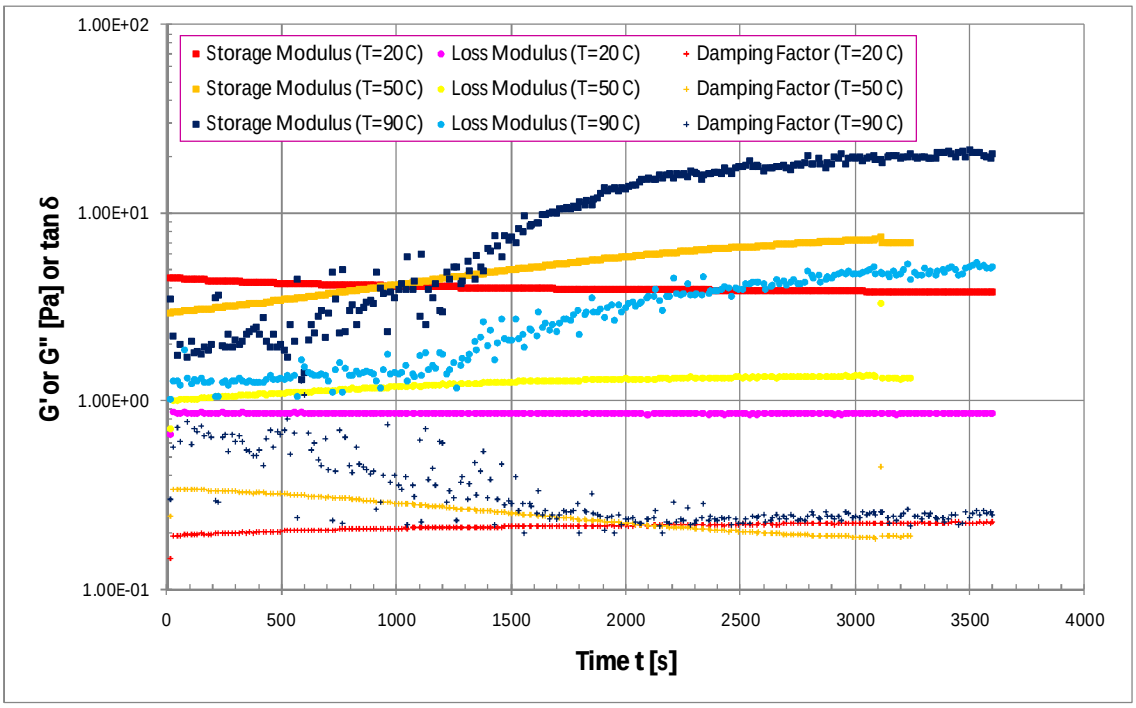

Figure 27 *Time test oscillation result for fracturing fluid 2 at 20, 50, and 90°C with 10% amplitude strain. G', G", and tan δ versus time.*

Time test oscillation measurements have also been performed for fracturing fluid 2. In these measurements, the fracturing fluid 2 was subjected to steady strain of 10%, angular frequency 10 1/s, and variation in temperature (20, 50, and 90°C). The results are presented in Fig. 27. It can be seen from Fig. 27, there is no intersection between G' and G" curves. However, G'

curve displays sudden rise after approximately 1000 s at 90°C. It might be the sign of the sol/gel transition point for this fracturing fluid (Romero-Zeron et al. 2004).

4.4 Temperature Test Oscillation

The following measurements in this chapter examine the temperature-dependent behavior of samples undergoing a chemical change during the test period.

Two measurements were conducted with fracturing fluid 1. In these measurements, the fracturing fluid samples were subjected to angular frequency 10 1/s and steady strain of 5% and 10%, respectively. As discussed earlier, the difference in amplitude strain should not affect the results as long as within the LVE range. The results, gathered in Fig. 28, show that the curves are fit enough (as was expected) until temperature 74°C after which the G' curves are different. This deviation could be due to instability of the measuring environment.

Observing Fig. 28, the 'reaction temperature' at which the chemical reaction with cross-linking or hardening begins can be obtained. At this conditions, the G' curve shows minimum values (Mezger 2002). In the view of Fig. 28, the reaction temperature for this fracturing fluid is approximately 74°C. With further heating, the G'(T) and G"(T) curves both increase. At higher temperatures, it can be expected to show a little softening (G' and G" curves decrease with slightly slope) due to heating up of the already hardened sample (Mezger 2002). However, it cannot be shown here due to temperature limitation of the measuring device.

From Fig. 28, it can be seen that the fracturing fluid is in gel state (solid state, with G' > G") below 60°C. Above 60°C, the fracturing fluid is in sol state (liquid state, with G" > G'). The fracturing fluid shows sol state only until 78°C above which it turns to gel state. The temperature at which the G' and G" curves intersect is called the sol/gel transition temperature or gel temperature or gel point (Mezger 2002). The sol/gel transition temperature for fracturing fluid 1 is approximately 78°C. At this temperature G' = G" or tan $\delta = 1$. The melting temperature at approximately 60°C is also noticeable in Fig. 28.

Another information from this measurement is temperature-dependent complex viscosity $|\eta^*(T)|$ of the fracturing fluid sample which are presented in Fig. 29. It can be seen from Fig. 29 that the viscosity minimum $|\eta^*_{min}|$ of fracturing fluid 1 is approximately 5.5E-2 Pas at temperature 74°C.

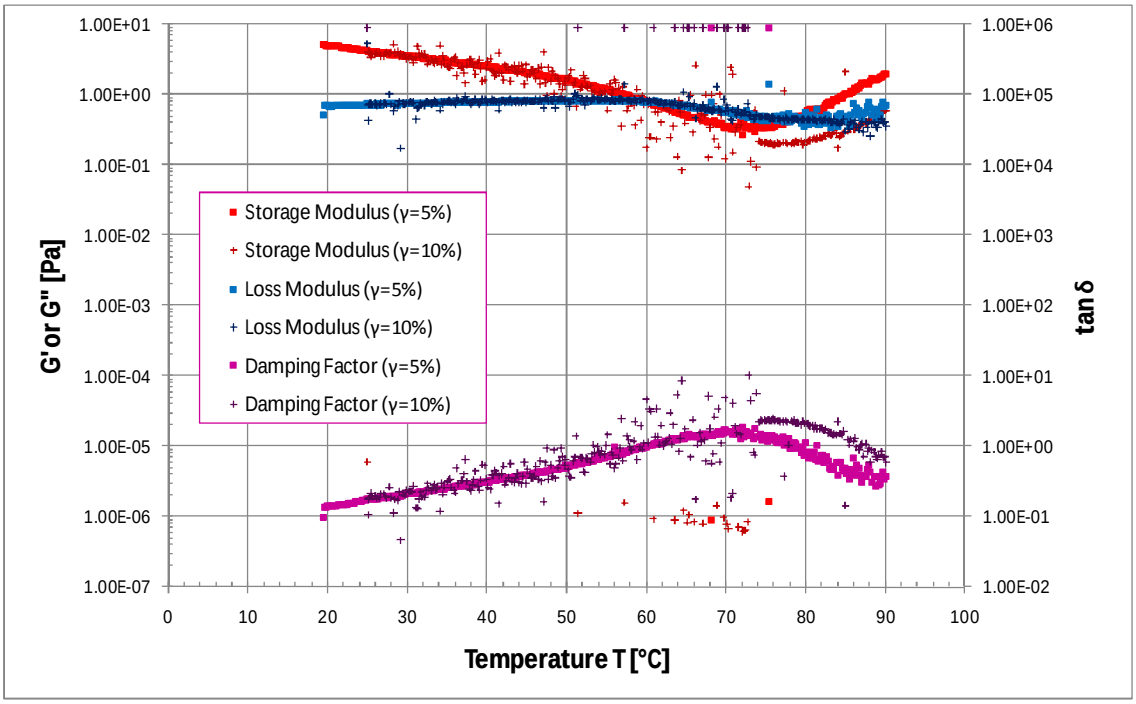

Figure 28 *Temperature test oscillation result for fracturing fluid 1 at angular frequency 10 1/s and amplitude strain of 5% and 10%. G', G", and tan δ versus temperature.*

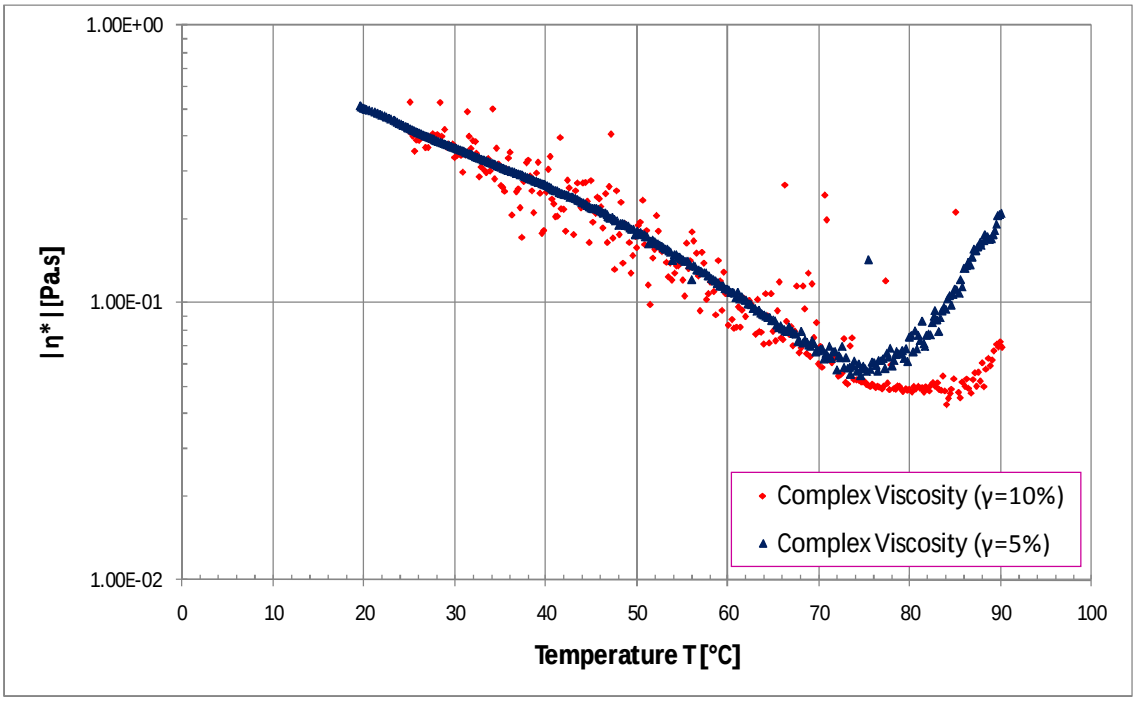

Figure 29 *Complex viscosity versus temperature for fracturing fluid 1.*

Temperature test oscillation measurements have also been performed for fracturing fluid 2 with two intervals where amplitude strains were 5% and 10%, respectively. In those measurements, the fracturing fluid samples were subjected to angular frequency 10 1/s. The results from those measurements, gathered in Fig. 30, show that the curves are fit enough as was expected.

It can be seen from Fig. 30, there is no intersection between G' and G" curves or the sol/gel transition temperature. However, in the view of Fig. 30, the hardening could be happened when G' displays sudden rise after 50°C (Romero-Zeron et al. 2004). At this temperature, the G' curve shows minimum values. Further heating at temperature above 65°C, it can be seen a little softening (G' and G" curves decrease with slightly slope) due to heating up of the already hardened sample (Mezger 2002).

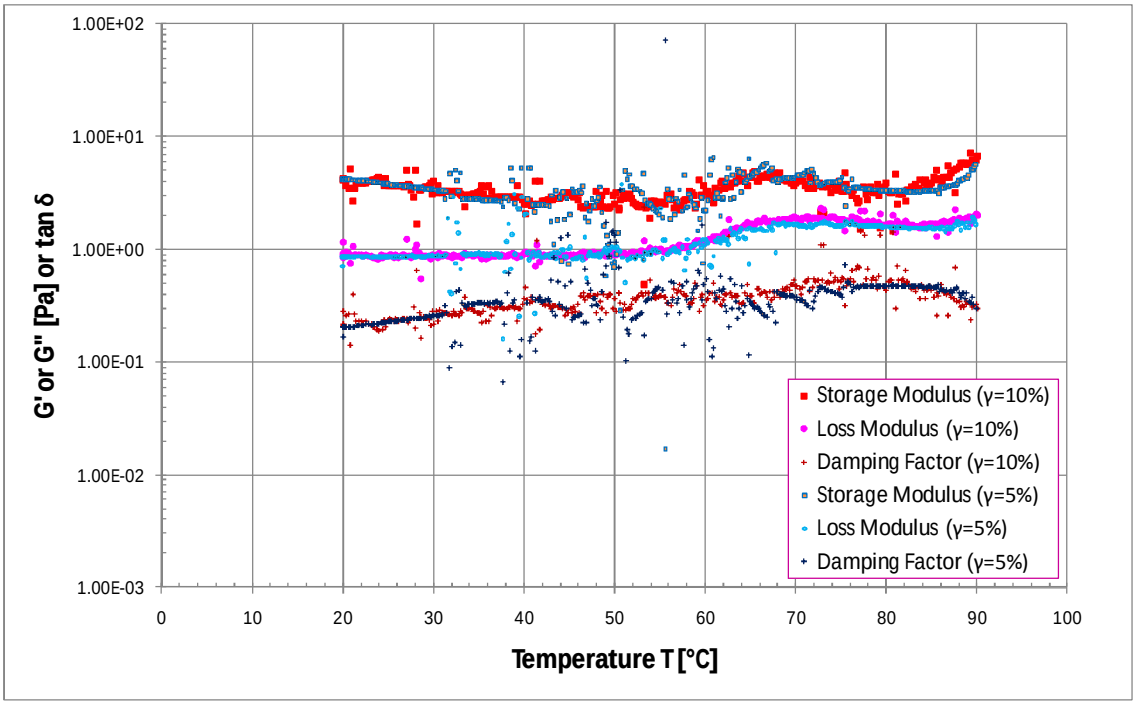

Figure 30 *Temperature test oscillation result for fracturing fluid 2 at angular frequency 10 1/s and amplitude strain of 5% and 10%. G', G", and tan δ versus temperature.*

In Fig. 31, the complex viscosity is plotted versus temperature. It can be observed from Fig. 31 that the viscosity minimum $|\eta^*_{min}|$ of fracturing fluid 2 is approximately 2.4E-1 Pas at temperature 55°C.

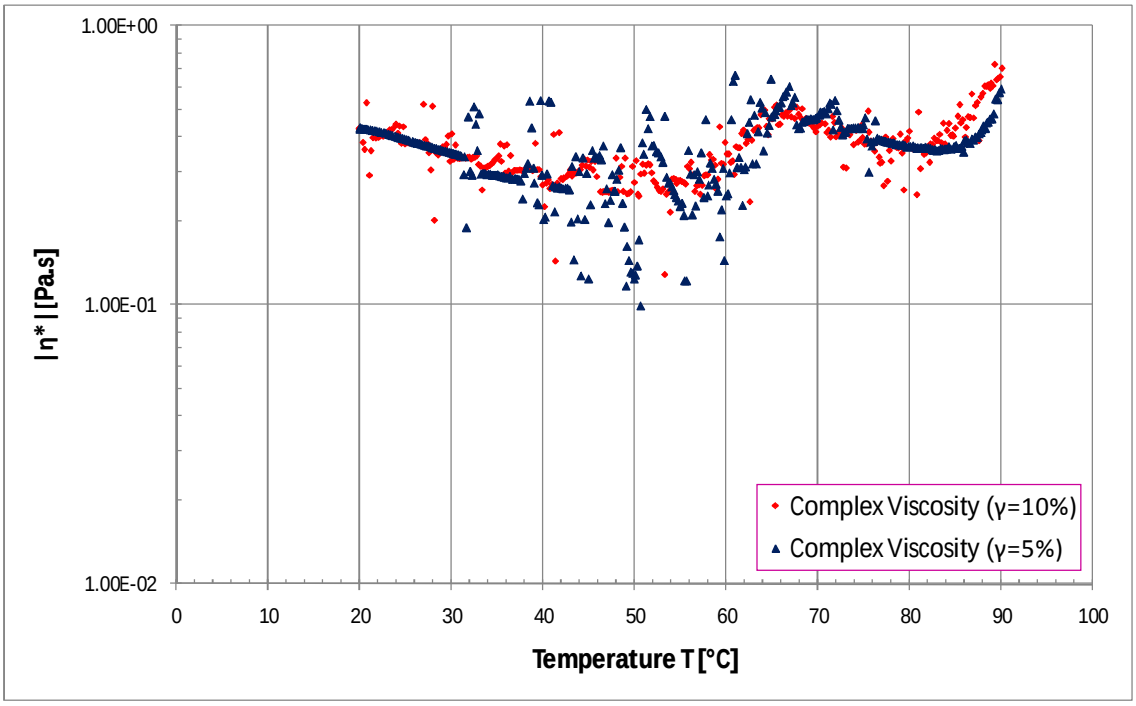

Figure 31 *Complex viscosity versus temperature for fracturing fluid 2.*

Nevertheless, it is important to mention the limitations and conditions that might affect the experiment. The experiments were performed in 'open system' that could be affected by outside temperature. It is suggested to perform the experiment in 'close system' if possible.

The fracturing fluids in this experiment might undergo chemical modification with time. One of these chemical instabilities is known as syneresis. Syneresis causes shrinkage in gel volume and consequently water is expelled from the gel structure (Romero-Zeron et al. 2004). This could result in non-homogeneous in the sample mixture. There were also lumps observed in the sample.

CONCLUSION

Oscillatory measurements have been performed to investigate the behavior of the rheological properties of the borate crosslinked fracturing fluids and the possible relationship among them. The main results are as follows:

- The amplitude sweep measurements show the temperature-dependence of the LVE limit. The plot of the LVE limit versus temperature in semi-logarithmic diagram is reasonably straight line.
- Storage modulus and loss modulus are independent of amplitude strain at LVE region.
- It was demonstrated that frequency sweep can differentiate a number of specific regions of the fracturing fluids in the viscoelastic spectrum (the viscous or terminal region, the transition to flow region, the rubbery or plateau region, the leathery or higher transition crossover region, and the glassy region).
- The flow-point frequency of the fracturing fluids is dependent on temperature. It increases exponentially with temperature.
- The gel points (time and temperature) are observable using time and temperature test oscillation.
- Additional information on the structural character of fracturing fluid can be obtained from G' and G" curves. It means that viscosity is inadequate in describing fracturing fluids.

REFERENCES

Bale, A., Larsen, L., Barton, D. T., and Buchanan, A. 2001. *Propped Fracturing as a Tool for Prevention and Removal of Formation Damage*. Paper SPE 68913 presented at the SPE European Formation Damage Conference, The Hague, The Netherlands, 21-22 May.

Barnes, H. A. 2000. *A handbook of elementary rheology*. Aberystwyth: Univ. of Wales, Institute of Non-Newtonian Fluid Mechanics.

Barnes, H. A., Hutton, J. F., and Walters, K. 1989. *An introduction to rheology*. Amsterdam: Elsevier.

Economides, M. J. 2007. *Modern Fracturing Enhancing Natural Gas Production*. Houston: Energy Tribune Publishing Inc.

Economides, M. J. and Nolte, K. G. 2000. *Reservoir stimulation*. Chichester: Wiley.

Fink, J. K. 2003. *Oil field chemicals*. Amsterdam: Gulf Professional Publ.

Friehauf, K. E. and Sharma, M. M. 2009. *Fluid Selection for Energized Hydraulic Fractures*. Paper SPE 124361 presented at the SPE Annual Technical Conference and Exhibition, New Orleans, Louisiana, USA, 4-7 October.

Friehauf, K. E., Suri, A., and Sharma, M. M. 2009. *A Simple and Accurate Model for Well Productivity for Hydraulically Fractured Wells*. Paper SPE 119264 presented at the SPE Hydraulic Fracturing Technology Conference, The Woodlands, Texas, USA, 19-21 January.

Gidley, J. L., Holditch, S. A., Nierode, D. E., and Veatch Jr., R. W. 1989. *Recent advances in hydraulic fracturing*. Monograph Series. New York: SPE.

Goel, N., Willingham, J. D., Shah, S. N., and Lord, D. L. 1997. *A Comparative Study of Borate-Crosslinked Gel Rheology Using Laboratory and Field Scale Fracturing Simulations*. Paper SPE 38618 presented at the SPE Annual Technical Conference and Exhibition, San Antonio, Texas, USA, 5-8 October.

Guo, B., Lyons, W. C., and Ghalambor, A. 2007. *Petroleum production engineering: a computer-assisted approach*. Amsterdam: Elsevier.

Guo, B., Sun, K., and Ghalambor, A. 2008. *Well productivity handbook: vertical, fractured, horizontal, multilateral, and intelligent wells*. Houston, Tex.: Gulf Publ. Co.

Harris, P. C. 1993. Chemistry and Rheology of Borate-Crosslinked Fluids at Temperatures to 300^{o}F. *SPE Journal of Petroleum Technology, 45*(3), 264-269.

Harris, P. C. and Heath, S. J. 1998. Rheological Properties of Low-Gel-Loading Borate Fracture Gels. *SPE Production & Operations, 13*(4), 230-235.

Huang, T. and Crews, J. B. 2007. *Nanotechnology Applications in Viscoelastic Surfactant Stimulation Fluids*. Paper SPE 107728 presented at the European Formation Damage Conference, Scheveningen, The Netherlands, 30 May-1 June.

Kesavan, S., Prud'homme, R. K., and Parris, M. D. 1993. *Crosslinked Borate HPG Equilibria and Rheological Characterization*. Paper SPE 25205 presented at the SPE International Symposium on Oilfield Chemistry, New Orleans, LA, USA, 2-5 March.

Mezger, T. G. 2006. *The rheology handbook: for users of rotational and oscillatory rheometers*. Hannover: Vincentz Verlag.

Mezger, T. G. 2002. *The rheology handbook: for users of rotational and oscillatory rheometers*. Hannover: Vincentz Verlag.

Penny, G. S., Pursley, J. T., and Holcomb, D. 2005. *The Application of Microemulsion Additives in Drilling and Stimulation Results in Enhanced Gas Production*. Paper SPE 94274 presented at the SPE Production Operations Symposium, Oklahoma City, OK, USA, 17-19 April.

Romero-Zeron, L., Manalo, F., and Kantzas, A. 2008. Characterization of Crosslinked Gel Kinetics and Gel Strength by Use of NMR. *SPE Reservoir Evaluation & Engineering, 11*(3), 439-453.

Romero-Zeron, L., Manalo, F., and Kantzas, A. 2004. *Characterization of Crosslinked Gel Kinetics and Gel Strength Using NMR*. Paper SPE 86548 presented at the SPE International Symposium and Exhibition on Formation Damage Control, Lafayette, Louisiana, USA, 18-20 February.

Shah, S. N., Lord, D. L., and Rao, B. N. 1997. *Borate-Crosslinked Fluid Rheology Under Various pH, Temperature, and Shear History Conditions*. Paper SPE 37487 presented at the SPE Production Operations Symposium, Oklahoma City, Oklahoma, USA, 9-11 March.

Shah, S. N., Lord, D. L., and Tan, H. C. 1992. *Recent Advances in the Fluid Mechanics and Rheology of Fracturing Fluids*. Paper SPE 22391 presented at the International Meeting on Petroleum Engineering, Beijing, China, 24-27 March.

Sinclair, A. R. 1970. Rheology of Viscous Fracturing Fluids. *SPE Journal of Petroleum Technology, 22*(6), 711-719.

Walters, H. G., Morgan, R. G., and Harris, P. C. 2001. *Kinetic Rheology of Hydraulic Fracturing Fluids*. Paper SPE 71660 presented at the SPE Annual Technical Conference and Exhibition, New Orleans, Louisiana, USA, 30 September-3 October.

Young, N. W. G., Williams, P. A., Meadows, J., and Allen, E. 1998. *A Promising Hydrophobicaly-Modified Guar for Completion Applications*. Paper SPE 39700 presented at the SPE/DOE Improved Oil Recovery Symposium, Tulsa, Oklahoma, 19-22 April.

Zolotukhin, A., Risnes, R., and Mishchenko, I. T. 2005. *Performance of Oil and Gas Wells*. Stavanger: University of Stavanger.

APPENDICES

APPENDIX A - Amplitude Sweep

Fracturing Fluid 1

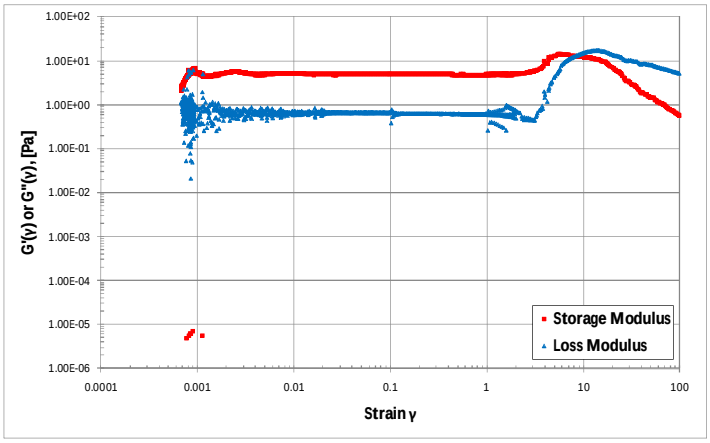

Figure 32 *G' and G" curves versus strain for fracturing fluid 1 at 20°C.*

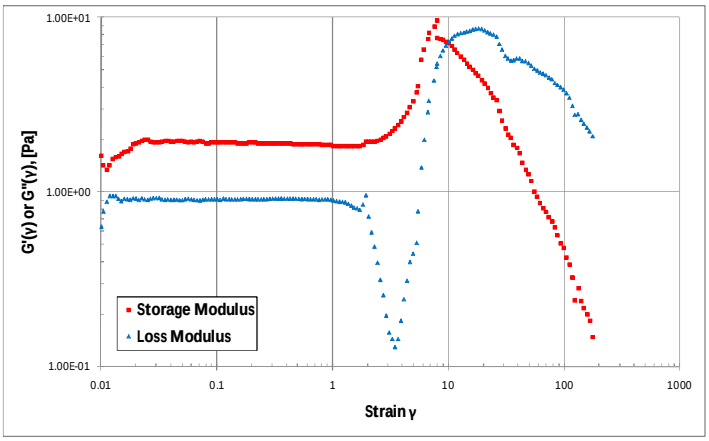

Figure 33 *G' and G" curves versus strain for fracturing fluid 1 at 40°C.*

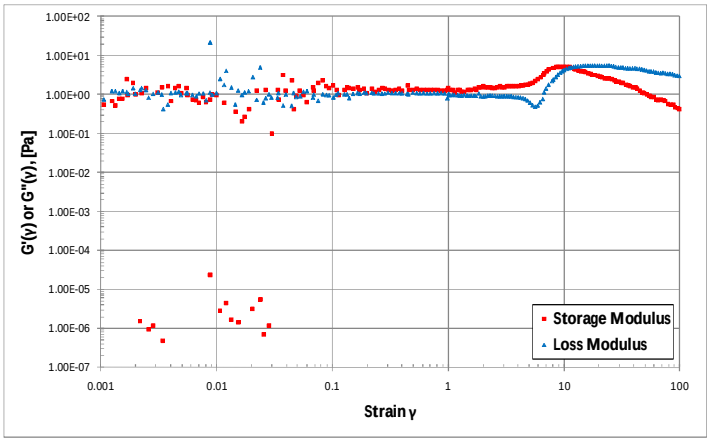

Figure 34 *G' and G" curves versus strain for fracturing fluid 1 at 50°C.*

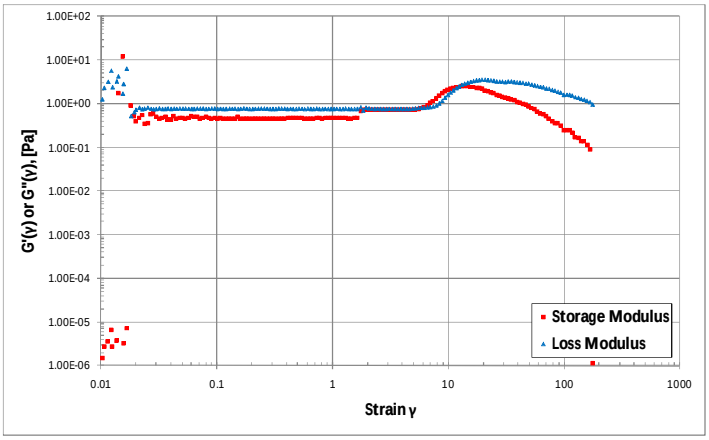

Figure 35 *G' and G" curves versus strain for fracturing fluid 1 at 60°C.*

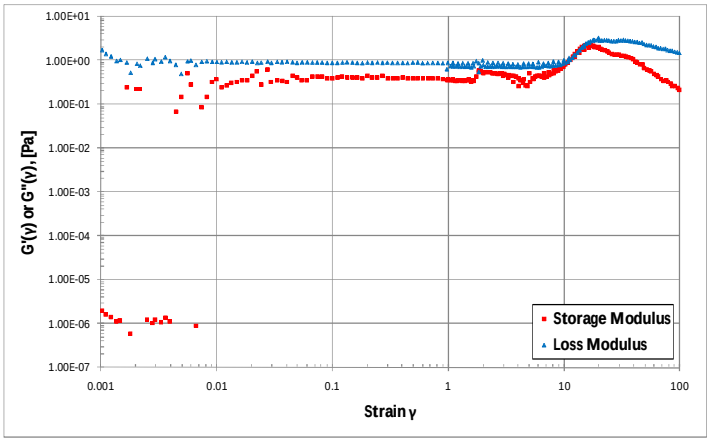

Figure 36 *G' and G" curves versus strain for fracturing fluid 1 at 70°C.*

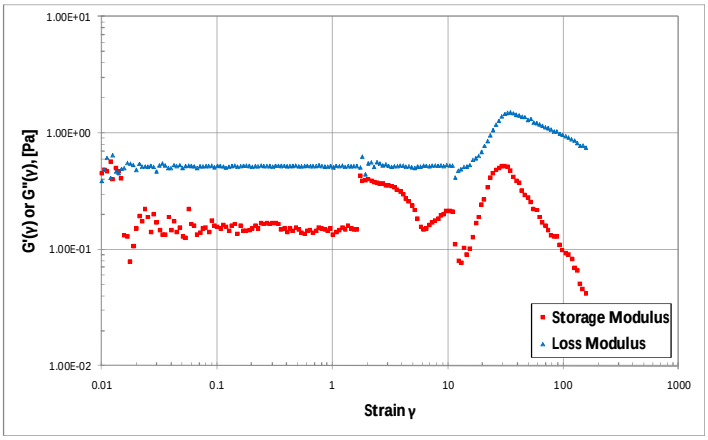

Figure 37 *G' and G" curves versus strain for fracturing fluid 1 at 80°C.*

Fracturing Fluid 2

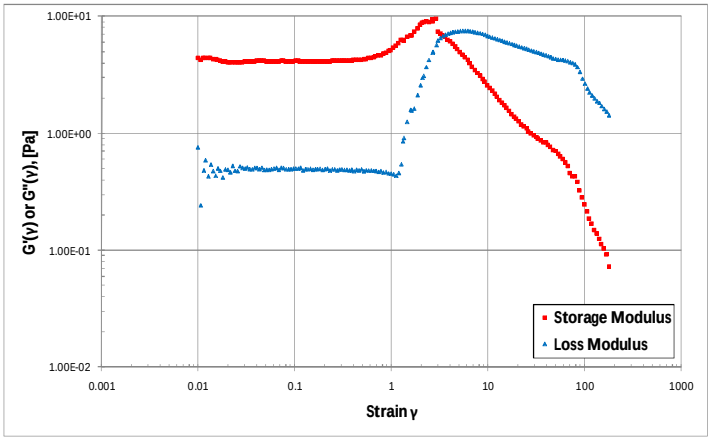

Figure 38 *G' and G" curves versus strain for fracturing fluid 2 at 20°C.*

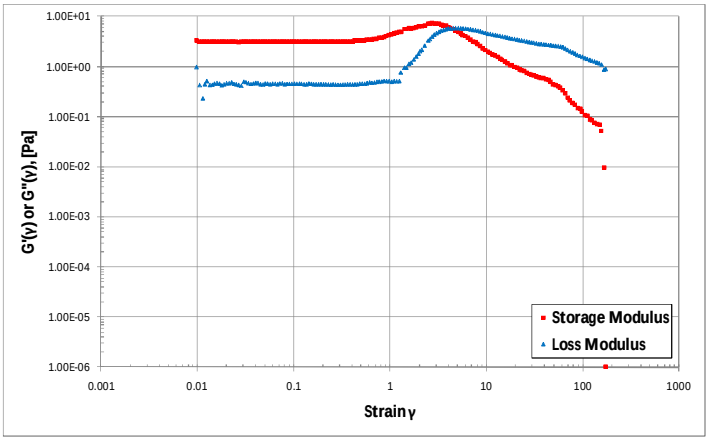

Figure 39 *G' and G" curves versus strain for fracturing fluid 2 at 30°C.*

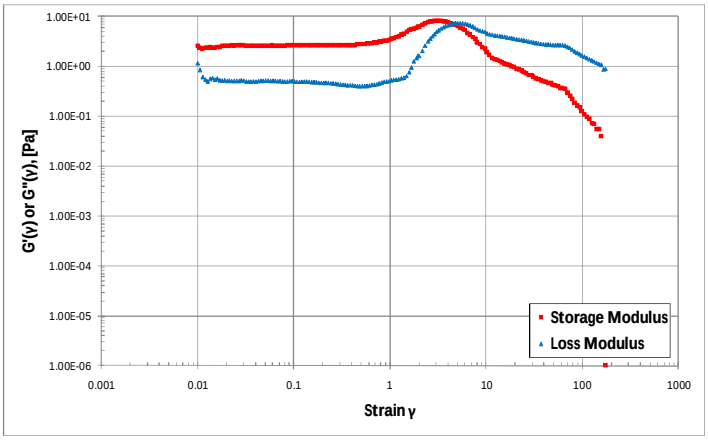

Figure 40 *G' and G" curves versus strain for fracturing fluid 2 at 40°C.*

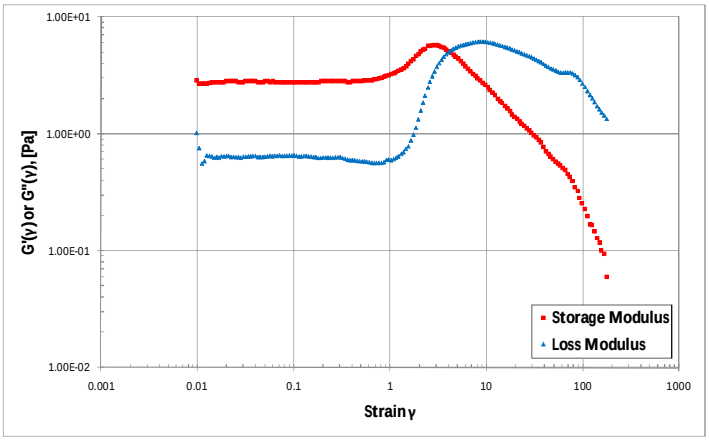

Figure 41 *G' and G" curves versus strain for fracturing fluid 2 at 50°C.*

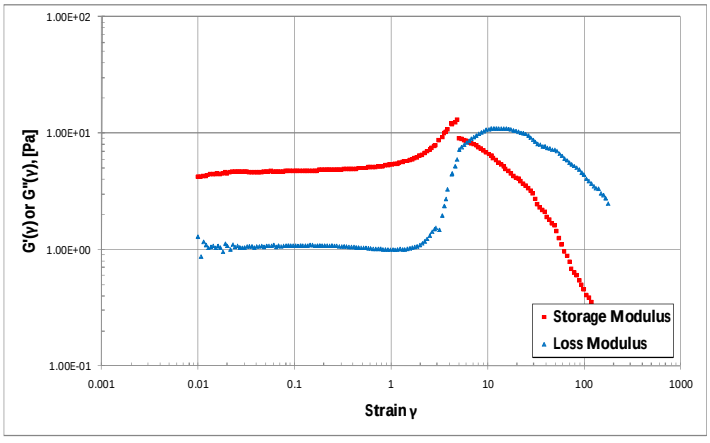

Figure 42 *G' and G" curves versus strain for fracturing fluid 2 at 60°C.*

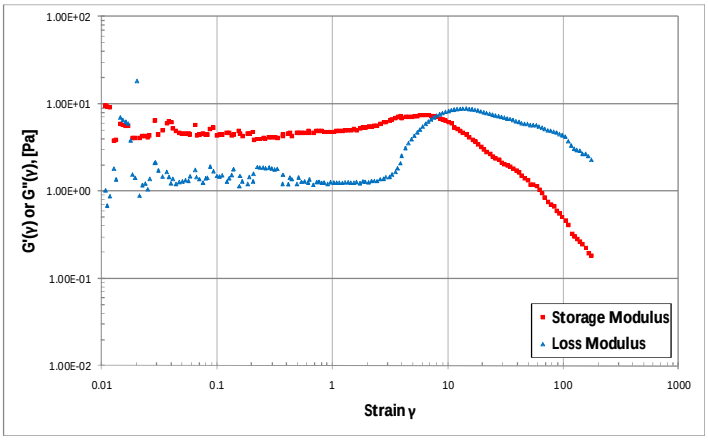

Figure 43 *G' and G" curves versus strain for fracturing fluid 2 at 70°C.*

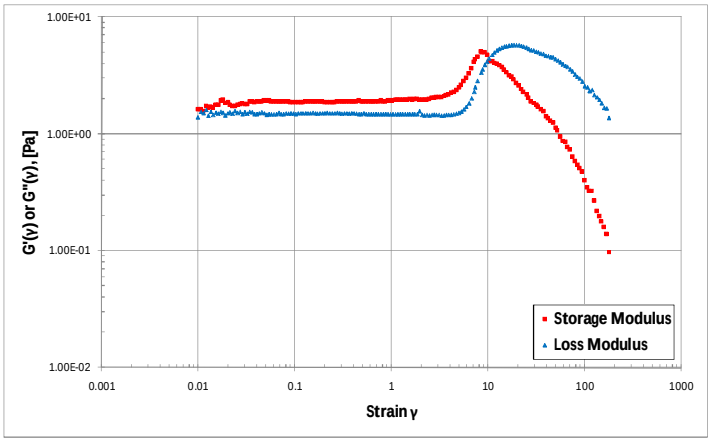

Figure 44 *G' and G" curves versus strain for fracturing fluid 2 at 90°C.*

APPENDIX B - Frequency Sweep

Fracturing Fluid 1

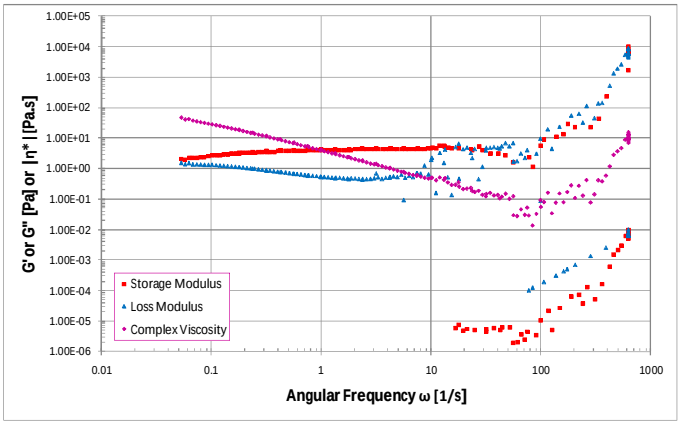

Figure 45 *Frequency sweep result for fracturing fluid 1 at 5% strain and 20°C.*

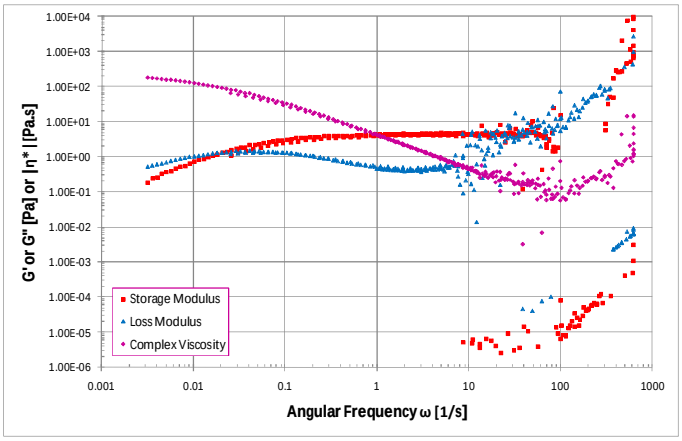

Figure 46 *Frequency sweep result for fracturing fluid 1 at 10% strain and 20°C.*

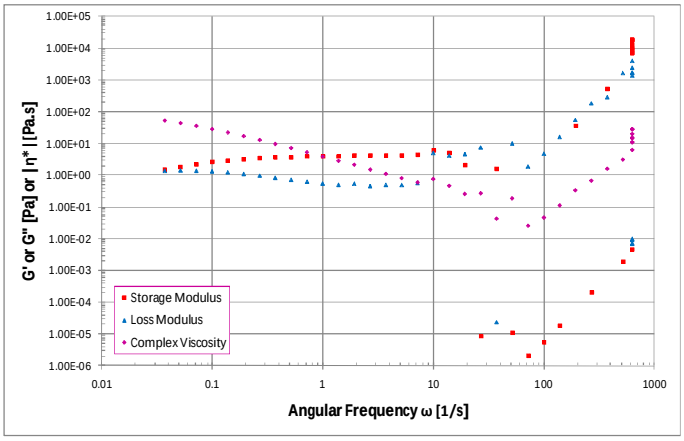

Figure 47 *Frequency sweep result for fracturing fluid 1 at 50% strain and 20°C.*

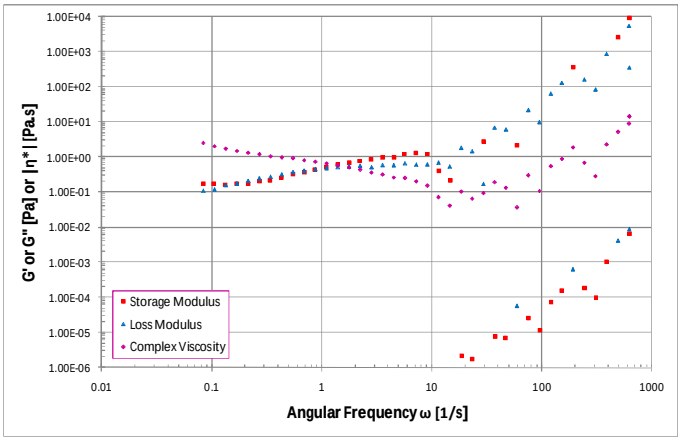

Figure 48 *Frequency sweep result for fracturing fluid 1 at 10% strain and 50°C.*

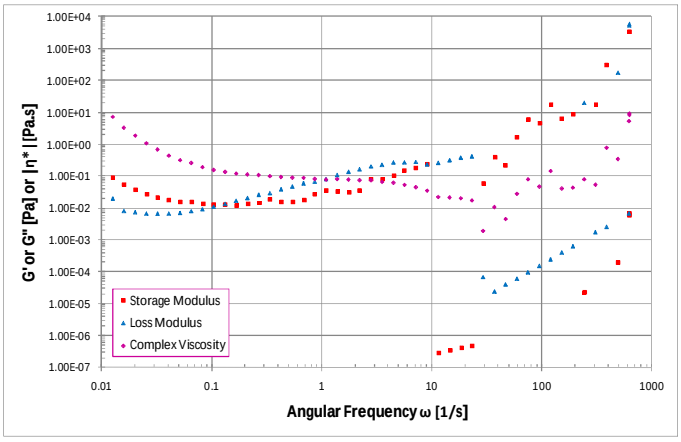

Figure 49 *Frequency sweep result for fracturing fluid 1 at 10% strain and 70°C.*

Fracturing Fluid 2

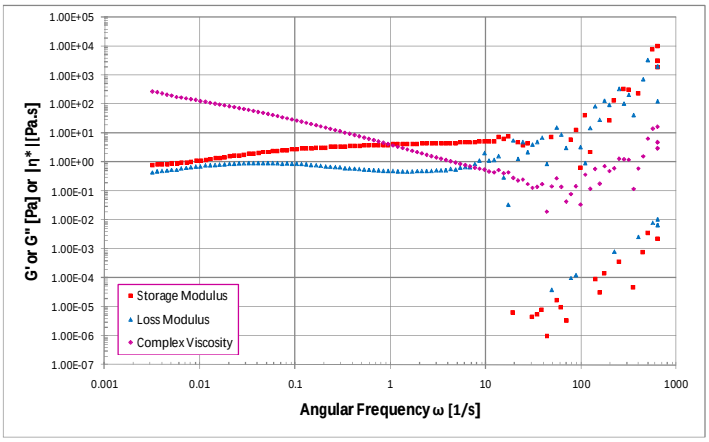

Figure 50 *Frequency sweep result for fracturing fluid 2 at 10% strain and 20°C.*

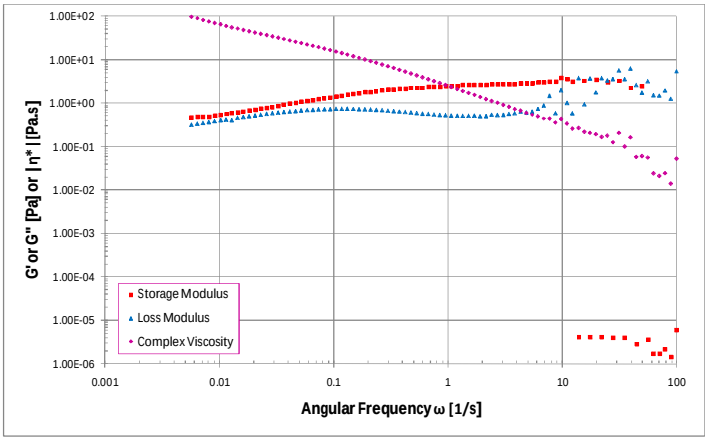

Figure 51 *Frequency sweep result for fracturing fluid 2 at 10% strain and 30°C.*

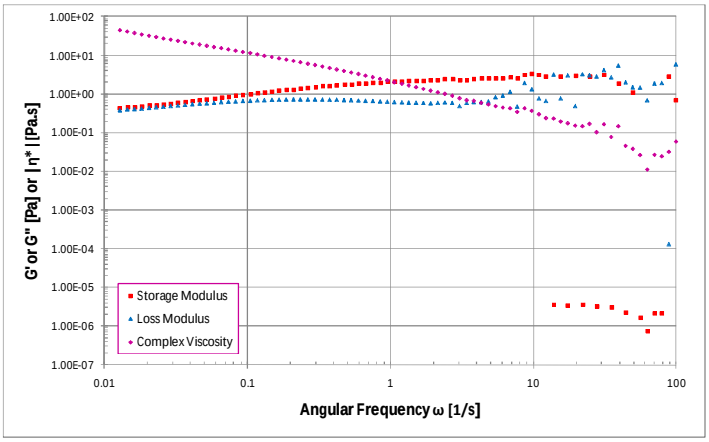

Figure 52 *Frequency sweep result for fracturing fluid 2 at 10% strain and 40°C.*

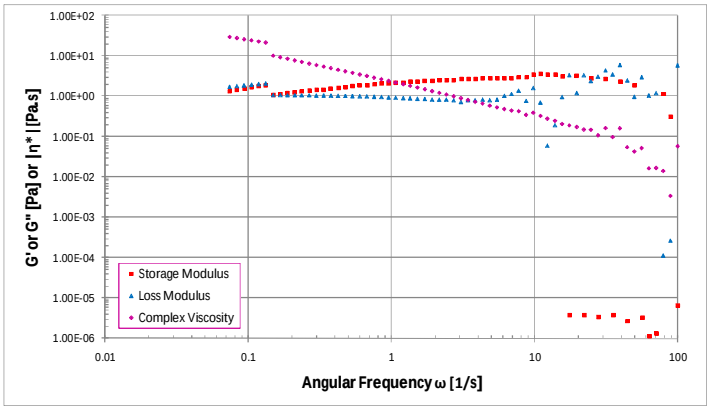

Figure 53 *Frequency sweep result for fracturing fluid 2 at 10% strain and 50°C.*

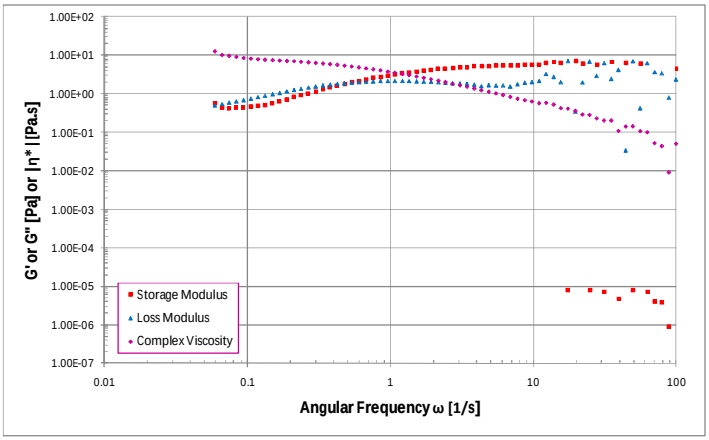

Figure 54 *Frequency sweep result for fracturing fluid 2 at 10% strain and 60°C.*

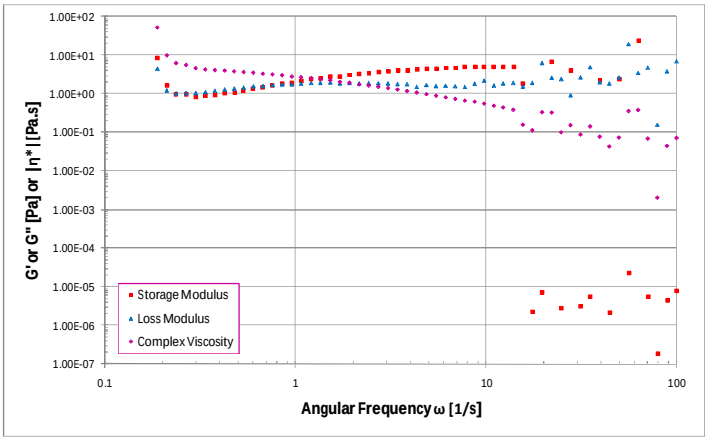

Figure 55 *Frequency sweep result for fracturing fluid 2 at 10% strain and 70°C.*

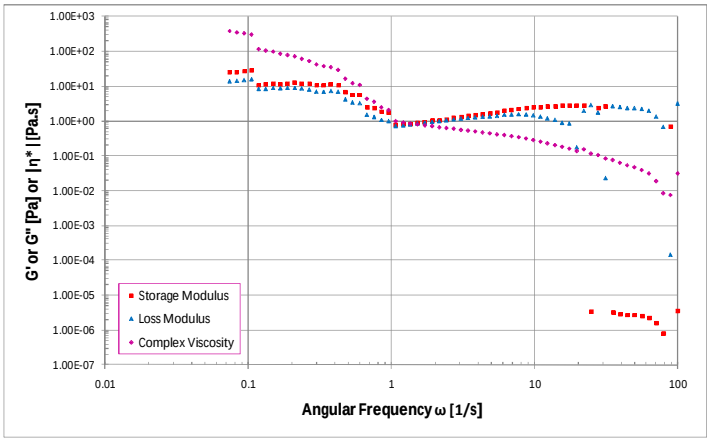

Figure 56 *Frequency sweep result for fracturing fluid 2 at 10% strain and 90°C.*

APPENDIX C - Summary of Measurements Setting

Table 2 *Summary of measurement setting for fracturing fluid 1*

TYPE OF MEASUREMENT	FIGURE NO.	INTERVAL	ANGULAR FREQUENCY [1/s]	AMPLITUDE STRAIN [%]	TEMPERATURE [deg C]	MEASURING SYSTEM	NUMBER OF DATA POINTS	MEASURING POINT DURATION [s]
Amplitude sweep	32	Interval 1	10	1E-3 - 10	20	Z3 DIN (25mm)	1,000	
		Interval 2	10	10 - 200	20	Z3 DIN (25mm)	200	
		Interval 3	10	100 - 1E+4	20	Z3 DIN (25mm)	200	
	33	Interval 1	10	1 - 1E+5	40	Z3 DIN (25mm)	200	
	34	Interval 1	10	0,1 - 100	50	Z3 DIN (25mm)	100	
		Interval 2	10	100 - 1E+4	50	Z3 DIN (25mm)	100	
	35	Interval 1	10	1 - 1E+5	60	Z3 DIN (25mm)	200	
	36	Interval 1	10	0,1 - 2000	70	Z3 DIN (25mm)	100	
		Interval 2	10	100 - 1E+4	70	Z3 DIN (25mm)	100	
	37	Interval 1	10	1 - 1E+5	80	Z3 DIN (25mm)	200	
Frequency sweep	45	Interval 1	100 - 0,1	5	20	Z3 DIN (25mm)	25	
		Interval 2	1E+4 - 1E-3	5	20	Z3 DIN (25mm)	200	
	46	Interval 1	100 - 0,01	10	20	Z3 DIN (25mm)	50	
		Interval 2	100 - 1E-3	10	20	Z3 DIN (25mm)	100	
		Interval 3	5 - 1E+3	10	20	Z3 DIN (25mm)	50	
		Interval 4	1 - 1E+3	10	20	Z3 DIN (25mm)	100	
	47	Interval 1	1E+4 - 1E-3	50	20	Z3 DIN (25mm)	50	
	48	Interval 1	1E+3 - 1E-2	10	50	Z3 DIN (25mm)	50	
	49	Interval 1	1E+3 - 1E-2	10	70	Z3 DIN (25mm)	50	
Time test oscillation	24	Interval 1	10	1	20	Z3 DIN (25mm)	240	30
		Interval 2	10	5	20	Z3 DIN (25mm)	240	30
		Interval 3	10	10	20	Z3 DIN (25mm)	120	30
	25	Interval 1	10	1	50	Z3 DIN (25mm)	60	15
		Interval 2	10	5	50	Z3 DIN (25mm)	60	15
		Interval 3	10	10	50	Z3 DIN (25mm)	60	15
	26	Interval 1	10	10	90	Z3 DIN (25mm)	200	15
Temperature test oscillation	28-29	Interval 1	10	10	25 - 90	Z3 DIN (25mm)	300	15
		Interval 2	10	5	20 - 90	Z3 DIN (25mm)	360	15

Table 3 *Summary of measurement setting for fracturing fluid 2*

TYPE OF MEASUREMENT	FIGURE NO.	INTERVAL	ANGULAR FREQUENCY [1/s]	AMPLITUDE STRAIN [%]	TEMPERATURE [deg C]	MEASURING SYSTEM	NUMBER OF DATA POINTS	MEASURING POINT DURATION [s]
Amplitude sweep	38	Interval 1	10	1 - 1E+5	20	Z3 DIN (25mm)	200	
	39	Interval 1	10	1 - 1E+5	30	Z3 DIN (25mm)	200	
	40	Interval 1	10	1 - 1E+5	40	Z3 DIN (25mm)	200	
	41	Interval 1	10	1 - 1E+5	50	Z3 DIN (25mm)	200	
	42	Interval 1	10	1 - 1E+5	60	Z3 DIN (25mm)	200	
	43	Interval 1	10	1 - 1E+5	70	Z3 DIN (25mm)	200	
	44	Interval 1	10	1 - 1E+5	90	Z3 DIN (25mm)	200	
Frequency sweep	50	Interval 1	1E+3 - 1E-3	10	20	Z3 DIN (25mm)	120	
	51	Interval 1	100 - 1E-3	10	30	Z3 DIN (25mm)	100	
	52	Interval 1	100 - 1E-3	10	40	Z3 DIN (25mm)	100	
	53	Interval 1	100 - 1E-3	10	50	Z3 DIN (25mm)	100	
	54	Interval 1	100 - 1E-3	10	60	Z3 DIN (25mm)	100	
	55	Interval 1	100 - 1E-3	10	70	Z3 DIN (25mm)	100	
	56	Interval 1	100 - 1E-3	20	90	Z3 DIN (25mm)	100	
Time test oscillation	27	Interval 1	10	10	20	Z3 DIN (25mm)	240	15
		Interval 2	10	10	50	Z3 DIN (25mm)	240	15
		Interval 3	10	10	90	Z3 DIN (25mm)	240	15
Temperature test oscillation	30-31	Interval 1	10	10	20 - 90	Z3 DIN (25mm)	360	15
		Interval 2	10	5	20 - 90	Z3 DIN (25mm)	360	15